

# **CRITICAL STATE MODELS AND THEIR COMPARISON WITH TRIAXIAL BEHAVIOR OF SOFT BANGKOK CLAY**

**S.R. Kim<sup>1</sup>, D.G. Lin<sup>2</sup>, D.T. Bergado<sup>3</sup>, A.S. Balasubramaniam<sup>4</sup>**

## **ABSTRACT**

Recently, the stress-strain behavior and the strength characteristics of Soft Bangkok Clay is studied in the triaxial apparatus under a variety of applied stress paths. The data are used to evaluate the potentials of the existing Critical State Theories in predicting soft clay behaviors and to determine the limitations of these which need improvements. In doing so, comparisons of the experimental behavior was also made with the Modified Cam Clay Theory (Roscoe & Burland, 1968; Pender's Theory, 1978; Dafalias Model, 1987; and Atkinson, 1987). Brief description of the theory are also given. Most of the behavior relates to the behavior below the State Boundary Surface and as such Pender's Model is used extensively in this paper for its capabilities in predicting soft clay behavior.

## **INTRODUCTION**

The Critical State Concept and associated stress-strain theories were developed based on experimental and analytical research undertaken from 1950 to 1970. These theories captured the bulk of the behavior of normally and overconsolidated clays as sheared from the isotropic pre-shear stress states with various degrees of accuracy.

The research is primarily aimed in undertaking an experimental study to evaluate the theoretical predictions for specimens sheared from  $K_0$  conditions both for normally and overconsolidated states of Bangkok clay. Thus the research work specially aims to:

1. experimentally study the behavior of Bangkok clay in the overconsolidated state (i.e., within the State Boundary Surface, SBS) and compare this behavior with the predictions from the existing stress-strain theories; and

---

1 Doctoral Engineering Graduate, School of Civil Engineering, Asian Institute of Technology, P.O.Box 4, Klong Luang, Pathumthani Province, Thailand.  
2 Assistant Professor of Geotechnical Engineering, School of Civil Engineering, Asian Institute of Technology, P.O.Box 4, Klong Luang, Pathumthani Province, Thailand.  
3 Professor of Geotechnical Engineering, School of Civil Engineering, Asian Institute of Technology, P.O.Box 4, Klong Luang, Pathumthani Province, Thailand.  
4 Chair Professor of Geotechnical Engineering, School of Civil Engineering, Asian Institute of Technology, P.O.Box 4, Klong Luang, Pathumthani Province, Thailand.

2. experimentally study the behavior of Bangkok clay in the normally consolidated state but sheared from  $K_o$  pre-shear consolidation conditions.

Pender (1978) extended the Cam Clay Theory based on the Critical State Concepts to predict the volumetric shear strains both below the SBS and on the SBS as sheared from isotropic and  $K_o$  pre-shear consolidation conditions. Thus, the experimental observations in this study will be compared extensively with Pender's Model (Pender, 1978) for the prediction of strains and pore pressures.

In making such comparisons with the theories, the Ko-consolidated behavior will also be studied in relation to the anisotropic stress-strain models of Pender (1977, 1978), Atkinson, et al., (1987) and Dafalias (1987), which all belong to the same family of Critical State Theories with varying degrees of modification. This study also proposes a conceptual modification of Pender's Model for the undrained behavior of lightly overconsolidated clays.

#### **CAMBRIDGE STRESS-STRAIN THEORIES FOR WET CLAYS BASED ON THE CRITICAL STATE CONCEPT**

The Cambridge Stress-Strain theories assume that the soil is isotropic, follow the Critical State Concept, and that there is no recoverable shear strain. The state of the stress inside the SBS must remain on the elastic wall which is a vertical plane above an isotropic swelling line. The plastic deformation is assumed to occur only when the state of the sample changes on the SBS.

The Cam-Clay model was developed for normally consolidated and lightly overconsolidated clay. The authors assumed that the energy dissipated at any infinitesimal increment of plastic work is only a function of the plastic shear strain. The proposed expression for energy dissipation with an assumption that the principal axes of stress and plastic strain increment coincide is,

$$dW = p d\varepsilon_{vp} + q d\varepsilon_{sp} = M p d\varepsilon_{sp} \quad (1)$$

where	$dW$	=	energy dissipated per unit volume of soil
	$p, q$	=	mean effective principal stress, deviator stress
	$d\varepsilon_{vp}, d\varepsilon_{sp}$	=	increments of plastic strains
	$M$	=	Stress ratio at critical state

## CRITICAL STATE MODELS

Burland (1965) proposed a modified work equation which considers the work dissipated in plastic volume change. The energy dissipated in the Modified Cam-Clay Model is,

$$dW = p [ (d\varepsilon_{vp})^2 + (Md\varepsilon_{sp})^2 ]^{1/2} \quad (2)$$

The flow rule and yield locus are given by Eqs. (3) and (4) respectively.

$$(d\varepsilon_{vp} / d\varepsilon_{sp}) = (M^2 - \eta^2) / 2\eta \quad (3)$$

$$p = (p_o M^2) / (M^2 + \eta^2) \quad (4)$$

Hence, the shape of the volumetric yield locus was changed from the earlier log spiral to an elliptic form.

The incremental shear and volumetric strains are as follows :

$$d\varepsilon_s = [(\lambda - \kappa) / (1 + e)] [2\eta / (M^2 - \eta^2)] [(2\eta d\eta / (M^2 + \eta^2) + (dp / p))] \quad (5)$$

$$d\varepsilon_v = [1 / (1 + e)] [2\eta (\lambda - \kappa) d\eta / (M^2 + \eta^2) + \lambda(dp / p)] \quad (6)$$

The State Boundary Surface described in this theory is

$$p / p_o = [M^2 / (M^2 + \eta^2)]^{(1-\lambda/\kappa)} \quad (7)$$

The Modified Theory of Roscoe and Burland (1968) captured many of the behavior of normally consolidated and lightly overconsolidated clays. Eq. (3) can make accurate predictions of  $K_o$ . Also Eq. (7) can predict the undrained stress paths and hence the pore pressures in normally and lightly overconsolidated clays.

The volumetric strains experienced by stress paths with states on the State Boundary Surface can be accurately determined using Eq. (6), while the shear strains as calculated from Eq. (5) are perfectly correct for the radial type of stress paths for which the stress ratio remain constant.

## PENDER'S MODEL (1977, 1978)

This model employed the Critical State Concept and a constitutive relationship for a work hardening plastic material as the general framework, and deals with two distinct behavior of clay, one for an overconsolidated behavior (Pender, 1978) and the other for the normally consolidated behavior (Pender, 1977).

### **Assumptions and Hypotheses**

While retaining most of the assumptions made in the Critical State Theory, the following aspects deviate from those.

1. Plastic strains occur within the State Boundary Surface. However, no unique State Boundary Surface is defined.
2. Two yield loci are engaged simultaneously when the stress path is directed outside the normally consolidated yield locus.

Hence, there exists three strains within the State Boundary Surface, i.e., the recoverable volumetric strain and the irrecoverable strains both volumetric and shear.

### **Summary of Pender's Model**

Whereas the Cambridge theories are concerned with behavior for stress states on the State Boundary Surface, Pender's Model is concerned not only with the behavior for stress paths beneath the State Boundary Surface but also with the behavior for the normally consolidated states. This model's great benefit is that it requires only four soil parameters which are obtainable from common laboratory tests. This model predicts fairly well the strength in the normally consolidated state, and hence, the undrained stress path as well because of the nature of the assumption of undrained stress paths. However, for the heavily overconsolidated state, the undrained stress paths are not supported by the real behavior. In spite of the drawbacks inherent in this model, it still provides the qualitative prediction of stress strain behavior of clays under the various initial stress conditions such as their behavior both in compression and in extension under the isotropic and anisotropic stress states. This model can also be extended to include the prediction of cyclic behavior of soils.

### **DAFALIAS' MODEL (1987)**

This model can be considered as an extended version of the classical Critical State Theory from an isotropic case to an anisotropic one. To include the effects of anisotropy induced by one dimensional stress states or other factors, Dafalias proposed a work equation including one additional term in that adopted by the Modified Cam Clay Theory of Roscoe and Burland (1968) as follows:

$$dW = p [ (d\varepsilon_{vp})^2 + (Md\varepsilon_{sp})^2 + 2\alpha d\varepsilon_{vp} d\varepsilon_{sp} ]^{1/2} \quad (8)$$

where  $\alpha$  is the triaxial non-dimensional anisotropic variable accounting for the effect of internal residual stresses.

## CRITICAL STATE MODELS

### Summary of Dafalias' Model

This model deals with the behavior of normally consolidated clay under anisotropic stress conditions. The yield surface proposed in this model consists of a rotated and distorted ellipse. The degree of rotation and distortion are determined by the value of  $\alpha$ .

A necessary condition of the work equation suggested is that:

$$2\alpha = 2\eta + (\eta^2 - M^2) (d\varepsilon_{sp} / d\varepsilon_{vp}) \quad (9)$$

If normality is assumed,  $\alpha$  is given by

$$\alpha = f(M, p, q, \beta) \quad (10)$$

where  $\beta$  is the memory function for the initial condition.

Thus, any assumption on the algebraic form of  $\alpha$  value has a direct impact on the shape of the yield surface. For instance,  $\alpha = 0$  (Modified Cam Clay Theory, Eq. 2) is a special case of a more general form of  $\alpha$ .

Dafalias did not extend this model to any type of incremental form of stress-strain behavior as is usually expected in the stress-strain theories.

### SOME FORMULATION OF ANISOTROPIC BEHAVIOR OF CLAYS

Atkinson, et al. (1987) proposed a State Boundary Surface for one-dimensionally normally consolidated clays based on the experimental data on reconstituted Speswhite Kaolin. These authors normalized all the test data with respect to the equivalent pressure,  $p_e$ , and the equivalent specific volume,  $v_\lambda$ , in order to take account of the different initial states and the different stress paths. The boundary surface which is normalized by  $v_\lambda$ , for one-dimensionally normally consolidated stress history is given as:

$$\eta - \eta_o = (\pm M - \eta_o) (2 \exp \{[(\Gamma - v_\lambda) / (\lambda - \kappa)]\})^{1/2} \quad (11)$$

where

$\eta_o$	=	stress ratio during one-dimensional consolidation
$\Gamma$	=	specific volume intercept of the Critical State line plotted as $v$ against $\ln p'$ at $p' = 1.0$

$$\begin{aligned} v_\lambda &= \text{Equivalent specific volume,} \\ &v_\lambda = v + \eta \ln p' \quad (v = \text{specific volume}) \\ M &= \text{stress ratio, } q/p, \text{ at Critical State} \end{aligned}$$

The State Boundary Surface was simply obtained by replacing  $\eta$  with  $(\eta - \eta_o)$  and  $M$  with  $(M - \eta_o)$  as the procedures adopted by the Modified Cam Clay Theory, when  $\eta_o = 0$ .

### COMMENTS ON VARIOUS MODELS

The energy balance equation proposed by Dafalias (1987) gives the most expression for the volumetric yield loci which lie on the State Boundary Surface. The Cam Clay Theory is the special version perhaps when the volumetric yielding is small, as it happens inside the State Boundary Surface. Therefore, the Cam Clay type of volumetric yield loci seem more reasonable to apply when the volumetric yield is small.

The volumetric yield loci, as obtained by Roscoe and Burland (1968), capture most of the behavior of normally consolidated clays as sheared from the isotropic stress state. With the suitable selection of  $\alpha$ , possibly the Dafalias' Model (1987) can apply for the anisotropic behavior of clays for stress states on the State Boundary Surface.

Pender's Model (Pender, 1977, 1978) based on experimentally observed undrained stress paths as parabolic idealization and the Critical State value of  $p_{cs}$  (the value of  $p$  at the point on the critical state line). When the model combined with an empirical flow rule, most of the type adopted for the Cam Clay Theory seems rather more complicated in its formulation. However, this model seems to capture the bulk of the clay behavior exhibited when stress paths lie below the State Boundary Surface.

These works indicate a need for the stress zone below the SBS to be investigated more closely for the existence of sub-sets of volumetric yield loci which can cause compressive volumetric strain on the wet side of the Critical State and dilatant volumetric strain on the dry side of the Critical State. It would then be necessary to seek appropriate flow rules in the stress regions where such sub-sets of volumetric yield loci exist. This is the major aim of the experimental program.

### EXPERIMENTAL INVESTIGATIONS

The behavior of normally and lightly overconsolidated clays was studied

## CRITICAL STATE MODELS

through a comprehensive series of triaxial tests. All test series were conducted on samples with OCR values of 1.00, 1.24, 1.50, 1.78, 2.15 and 2.75.

### Triaxial Consolidation Tests

In this study, the idealized  $K_o$ -swelling line was used for the preparation of overconsolidated specimens. It was defined in the  $p$ - $q$  stress space as the straight line in which the stress increment ratio is 0.95 passing through the normally consolidated stress point. Eventually, all of the final consolidation stress points of overconsolidated specimens fell on this idealized straight  $K_o$ -line.

In order to justify the idealized actual  $K_o$ -swelling line, four swelling tests (as shown in Table 1) were carried out with the different swelling stress increment ratio,  $|dq/dp| = 0.49, 0.82, 0.85$ , and  $0.95$  after  $K_o$ -consolidation. The schematic diagram of consolidation procedures is shown in Fig. 1. The slope of the consolidation and the swelling line in the  $e$ - $\ln p$  plot were  $0.357$  and  $0.081$ , respectively. These values were used for the preparation of overconsolidated clay specimens in the laboratory.

### Triaxial Test Series

A systematic triaxial test consisted of three test series, namely, Test Series I, II and III. Test Series I and II were the anisotropic tests, while the remaining one was isotropic tests. All initial stress points of each test series are illustrated in Table 2 and Fig. 2.

Detailed testing schedule is tabulated in Table 3 and typical stress paths are shown in Fig. 3.

**Table 1 Triaxial Consolidation Test**

Test Name	Number of Test	Consolidation Stress Ratio $\eta$	Swelling Stress Ratio Increment $ dq/dp $
CA-0.49	1	0.49	0.49
CA-0.82	1	0.49	0.82
CA-0.85	1	0.49	0.85
CA-0.95	1	0.49	0.95
CI-1,2,3	3	0	0
Total No. of Test	7		

**Note :**

CA = anisotropic Consolidation

CI = isotropic Consolidation

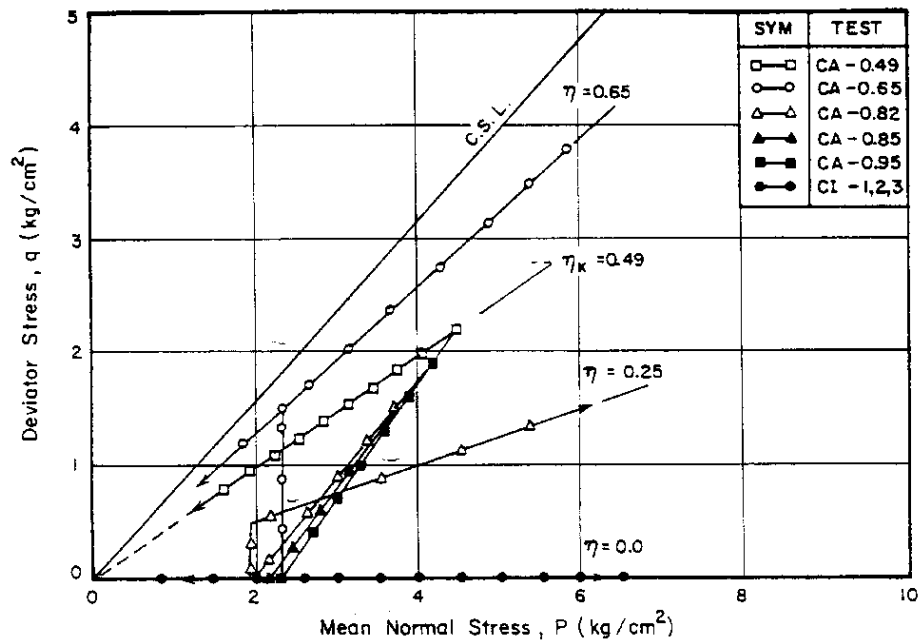


Fig. 1 Schematic Diagram of Consolidated Process

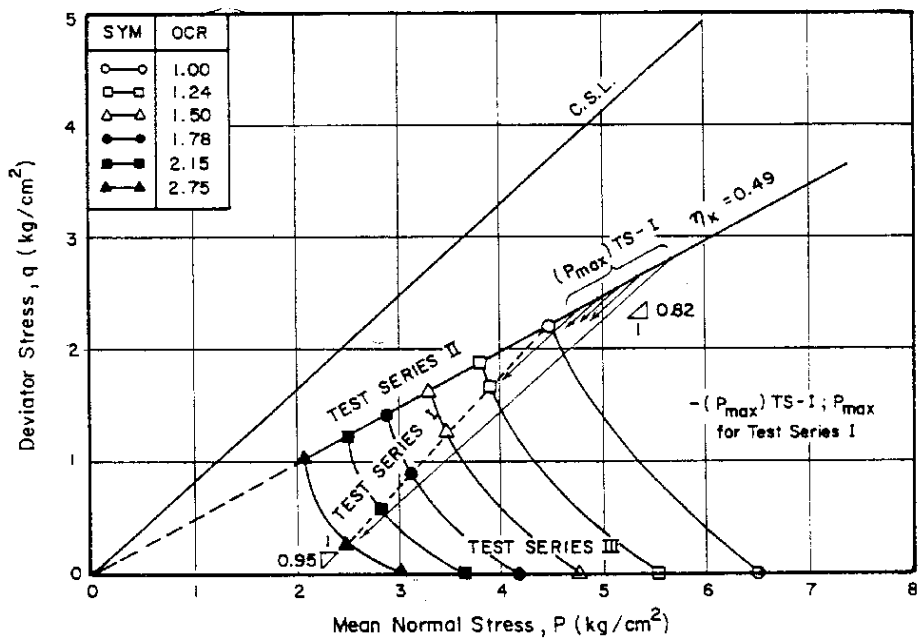


Fig. 2 Initial Stress Points of Test Series I, II, III



## CRITICAL STATE MODELS

**Table 2 Conditions for the Overconsolidated Samples in  $q$ - $p$  Stress Space**

OCR		TEST SERIES I					
$OCR$ ( $\bar{\sigma}_{vm} / \bar{\sigma}_{vo}$ )	$(OCR)_p$ $p_{max} / p_o$	$p_{max}$ (kg/cm <sup>2</sup> )	$q_{max}$ (kg/cm <sup>2</sup> )	$p_o$ (kg/cm <sup>2</sup> )	$q_o$ (kg/cm <sup>2</sup> )	$K_o$	$\eta$
1.00	1.00	4.500	2.205	4.500	2.205	0.63	0.49
1.24	1.20	4.690	2.298	3.908	1.657	0.67	0.42
1.50	1.40	4.857	2.380	3.469	1.242	0.71	0.36
1.78	1.60	5.006	2.453	3.129	0.914	0.76	0.29
2.15	1.85	5.174	2.535	2.797	0.586	0.82	0.21
2.75	2.20	5.382	2.637	2.446	0.230	0.91	0.09

OCR		TEST SERIES II					
$OCR$ ( $\bar{\sigma}_{vm} / \bar{\sigma}_{vo}$ )	$(OCR)_p$ $p_{max} / p_o$	$p_{max}$ (kg/cm <sup>2</sup> )	$q_{max}$ (kg/cm <sup>2</sup> )	$p_o$ (kg/cm <sup>2</sup> )	$q_o$ (kg/cm <sup>2</sup> )	$K_o$	$\eta_o$
1.00	1.00	4.500	2.205	4.500	2.205	0.63	0.49
1.24	1.24	4.725	2.315	3.811	1.867	0.63	0.42
1.50	1.50	4.934	2.418	3.289	1.612	0.63	0.49
1.78	1.78	5.129	2.513	2.882	1.412	0.63	0.49
2.15	2.15	5.354	2.623	2.490	1.220	0.63	0.49
2.75	2.75	5.661	2.774	2.059	1.009	0.63	0.49

OCR		TEST SERIES III					
$OCR$ ( $\bar{\sigma}_{vm} / \bar{\sigma}_{vo}$ )	$(OCR)_p$ $p_{max} / p_o$	$p_{max}$ (kg/cm <sup>2</sup> )	$q_{max}$ (kg/cm <sup>2</sup> )	$p_o$ (kg/cm <sup>2</sup> )	$q_o$ (kg/cm <sup>2</sup> )	$K_o$	$\eta_o$
1.00	1.00	6.500	0	6.500	0	1	0
1.24	1.24	6.840	0	5.516	0	1	0
1.50	1.50	7.155	0	4.770	0	1	0
1.78	1.78	7.451	0	4.186	0	1	0
2.15	2.15	7.792	0	3.624	0	1	0
2.75	2.75	8.260	0	3.004	0	1	0

**Notes :**

(OCR) = the ratio of the maximum past vertical stress to the pre-shear vertical stress

(OCR)<sub>p</sub> = the ratio of the maximum past mean normal stress to the pre-shear mean normal stress

**Table 3 Test Conditions and Test Names With Test Series**

TEST SERIES I				
Undrained Compression Tests	Undrained Extension Tests	Drained Compression Tests	Drained Extension Tests	Drained Extension Loading Tests
C Ko U1 C Ko U2 C Ko U3 C Ko U4 C Ko U5 C Ko U6 C Ko U1-2	C Ko UE1 C Ko UE2 C Ko UE3 C Ko UE4 C Ko UE5 C Ko UE6 C Ko UE1-2	C Ko D1 C Ko D2 C Ko D3 C Ko D4 C Ko D5 C Ko D6 -	C Ko DE1 C Ko DE2 C Ko DE3 C Ko DE4 C Ko DE5 C Ko DE6 -	- - - C Ko LE4 - C Ko LE6 -
Drained Compression Tests <i>p</i> -constant	Drained Extension Tests <i>p</i> -constant	Drained Loading Tests <i>q</i> -constant	Drained Unloading Tests <i>q</i> -constant	Drained Unloading Compression Tests
C Ko PC1 C Ko PC2 C Ko PC3 C Ko PC4 C Ko PC5 C Ko PC6	C Ko PE1 C Ko PE2 - C Ko PE4 - C Ko PE6	- C Ko QL2 C Ko QL3 - C Ko QL5 -	C Ko QU1 C Ko QU2 C Ko QU3 - C Ko QU5 -	C Ko DU1 C Ko DU2 C Ko DU3 - C Ko DU5 -

TEST SERIES II		TEST SERIES III	
Undrained Compression Tests	Drained Compression Tests	Undrained Compression Tests	Drained Compression Test
- CAU2 CAU3 CAU4 CAU5 CAU6	- CAD2 CAD3 CAD4 CAD5 CAD6	CIU1 CIU2 CIU3 CIU4 CIU5 CIU6 *CIU7 CIU1-2 CIU1-3	CID1 CID2 CID3 CID4 CID5 CID6

**Notes :**

(1) - : No Test is carried out.

(2) Numbers 1-6 in each test name denote OCRs of 1.0, 1.24, 1.5, 1.78, 2.15 and 2.75

(3) OCR for \*CIU7 is 4.25 and *p*' for CIU1-2 & CIU1-3 are 6.0 and 5.0 kg/m<sup>2</sup>

## CRITICAL STATE MODELS

### Compression Conditions

1.  $CK\sigma_U$ ,  $CAU$ ,  $CIU$  = Conventional undrained compression tests on  $K\sigma$  anisotropically, and isotropically consolidated specimens, i.e., increasing the axial stress with keeping the constant cell pressure (Test Series I, II & III)
2.  $CK\sigma_D$ ,  $CAD$ ,  $CID$  = Conventional drained compression tests on  $K\sigma$  anisotropically, and isotropically consolidated specimens. (Test Series I, II & III)
3.  $CK\sigma_{DU}$  = Unloading drained compression tests on  $K\sigma$ -consolidated specimens, i.e., decreasing radial stress with keeping the axial stress constant. (Test Series I)
4.  $CK\sigma_{PC}$  =  $p$ -constant drained compression tests on  $K\sigma$ -consolidated specimens. (Test Series I)
5.  $CK\sigma_{QL}$ ,  $CK\sigma_{QU}$  =  $q$ -constant drained loading and unloading on  $K\sigma$ -consolidated specimens. (Test Series I)

### Extension Conditions

6.  $CK\sigma_{UE}$ ,  $CK\sigma_{DE}$  = Conventional undrained and drained extension tests on  $K\sigma$ -consolidated specimens. (Test Series I)
7.  $CK\sigma_{LE}$  = Extension drained loading tests on  $K\sigma$ -consolidated specimens. (Test Series I)
8.  $CK\sigma_{PE}$  =  $p$ -constant drained extension tests on  $K\sigma$ -consolidated specimens. (Test Series I)

## INDEX PROPERTIES OF CLAY

The clay used in this study was retrieved from depths of between 3.0 m to 4.0 m (a narrow range) within the Asian Institute of Technology. The physical properties are summarized in Table 4.

**Table 4 Index Properties**

Natural Water Content (%)	78 – 85
Liquid Limit (%)	98
Plastic Limit (%)	37
Plasticity Limit (%)	61
Liquidity Index	0.67 – 0.79
Average Unit Weight ( $t/m^3$ )	1.51
Specific Gravity	2.69
Clay Content	70
Silt Content	24
Sand Content	6

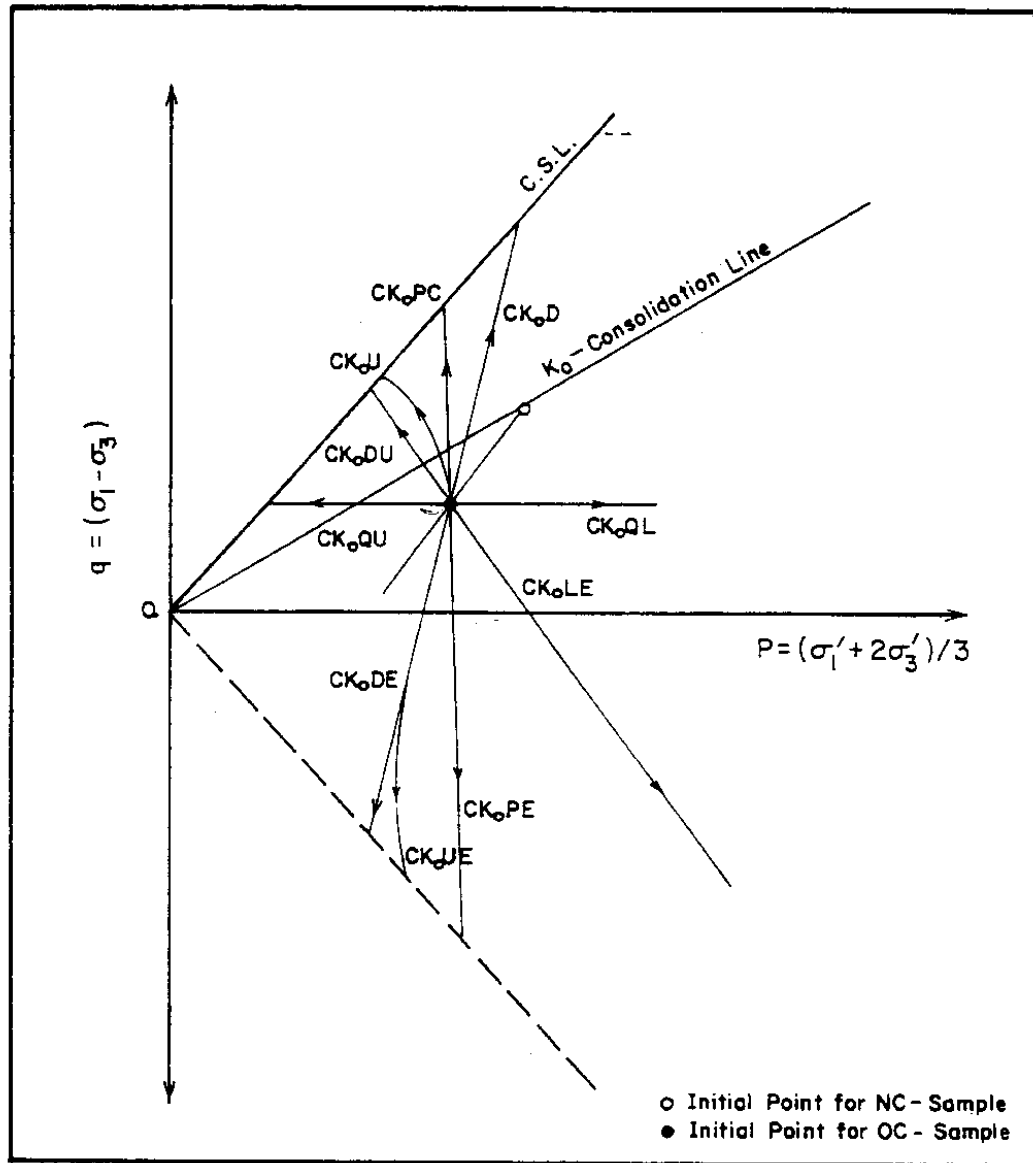


Fig. 3 Typical Stress Paths followed in this Investigation of the Behavior of Lightly Overconsolidated Clay (Test Series I)

### CONSOLIDATION CHARACTERISTICS OF CLAYS

Isotropic and anisotropic consolidation and swelling tests were conducted to study the consolidation and swelling characteristics. The stress ratio,  $\eta$ , in  $p$ - $q$  stress space for the  $K_0$  consolidation is 0.49 (since  $K_0$  is taken as 0.63) as determined by previous investigators at AIT (e.g., Chang, 1973; Chaiyadhuma, 1974; Wong, 1975).

## CRITICAL STATE MODELS

### Void Ratio- Pressure Relationships

The  $(e, \ln p)$  relationships of the isotropically and  $K_o$ -consolidated specimens are shown in Fig. 4.

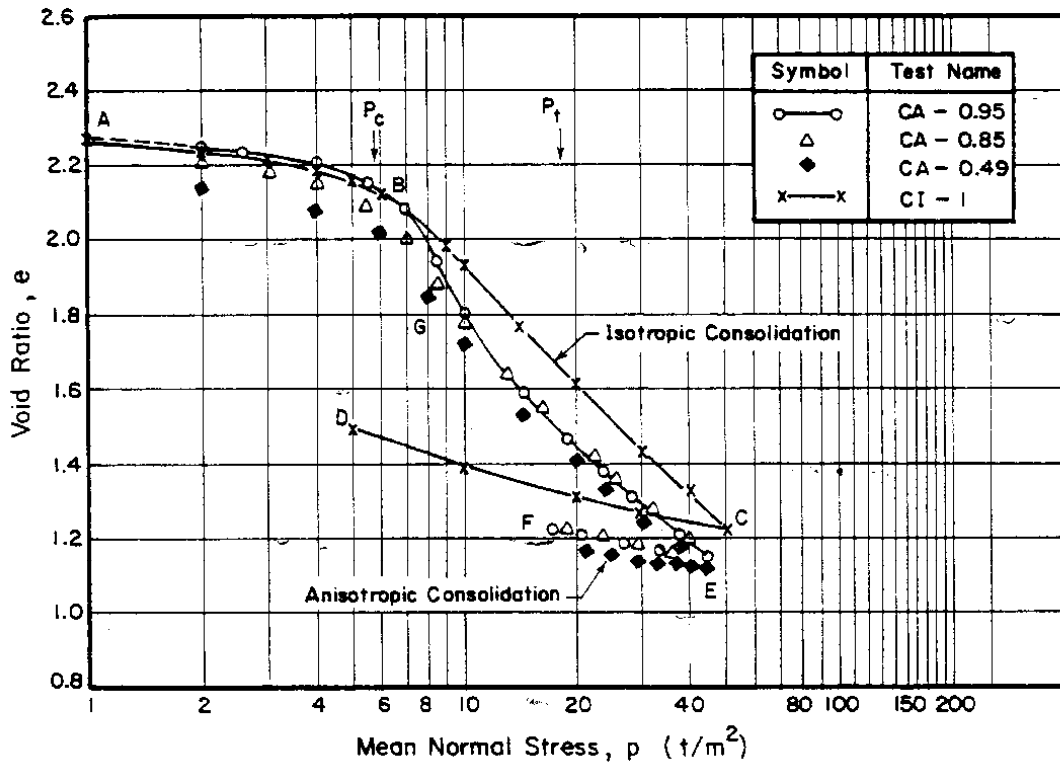


**Fig. 4 Typical Consolidation and Swelling Curves**

The ratio of  $(p_t / p_c)$  is about 3.3 and it seems that for consolidation pressures higher than about 3.3 times the initial pre-consolidation pressure, the effects of initial shear stress due to  $K_o$  consolidation can be erased. This value is quite close to that reported by Balasubramaniam (1969). The compression index,  $\lambda$  in the normally consolidated state at the higher stress level is 0.357 and this value together with the appropriate  $\kappa$  value of 0.081 was used in the preparation of overconsolidated samples.

### Swelling Characteristics

The plastic volumetric strain ratio  $\Lambda$ , defined as  $\Lambda = (1 - \kappa / \lambda)$  will be 0.77. This value is close to the value of 0.75-0.85 and 0.78 as reported by Ladd et al. (1977).

**COMPARISON OF UNDRAINED BEHAVIOR OF NORMALLY  
CONSOLIDATED CLAYS UNDER  $K_0$  PRE-SHEAR STRESS CONDITIONS**

**Effective Stress Paths**

The undrained stress paths for the  $K_0$ -normally consolidated state from different stress strain models are superimposed with the experimental data in Fig. 5.

1. **Triaxial Compression** - All model predictions deviate from the experimental observations, particularly, they fail to simulate the undrained stress path in the early stages of the loading. As stated earlier, these deviations may result since the sample exhibits the effects of secondary consolidation (gained during the consolidation phase in the sample preparation), while the models are not expected to include such time effects. Pender's Model seems to predict successfully the undrained stress path.
2. **Triaxial Extension** - All model predictions during the extension phase above the  $p$ -axis (i.e.,  $0 < \eta < \eta_r$ ) are reasonably coincident with the experimental observations. In the pure extension stress state, when  $\eta$  is less than zero, all model predictions deviate from the experimentally observed stress path. Pender's Model gives the best prediction for the extension condition. As reviewed studies, the mean effective normal stress for low plasticity clay during the extension phase is drastically reduced.

**Stress-Strain Relationships**

The stress-strain curves are shown in Figs. 6a, 6b, and 7.

1. **Triaxial Compression** - The prediction provided with the approach reported by Atkinson et al. (1987) significantly underpredicts the strength as expected from an undrained stress path. Pender's Model also underpredicts the strength and overpredicts the shear strain. However, the predictions obtained from Dafalias' Model agree well with the experimental data. It seems all models fail to simulate the stress-strain relationship in the early stages of loading; probably, because the experimental observations include time effects due to secondary consolidation.
2. **Triaxial Extension** - In the case of the extension tests, all model predictions agree well with the experimental data up to the  $p$ -axis. However, there are tendencies for Pender's Model to give larger strains, while the other two models give smaller shear strains at the same deviator stress level. Except Pender's Model, the other two models are relatively rigid in distortion for stress states less than the peak deviator stress. Upon approaching the peak deviator stress, these models show an abrupt increase in shear distortion similar to those patterns seen

## CRITICAL STATE MODELS

in the compression tests. Generally, Pender's Model, although it overpredicts the shear strains, reveals a qualitatively reasonable stress-strain relationship in the extension phase when the model parameters are determined from the peak deviator stress conditions (Fig. 7).

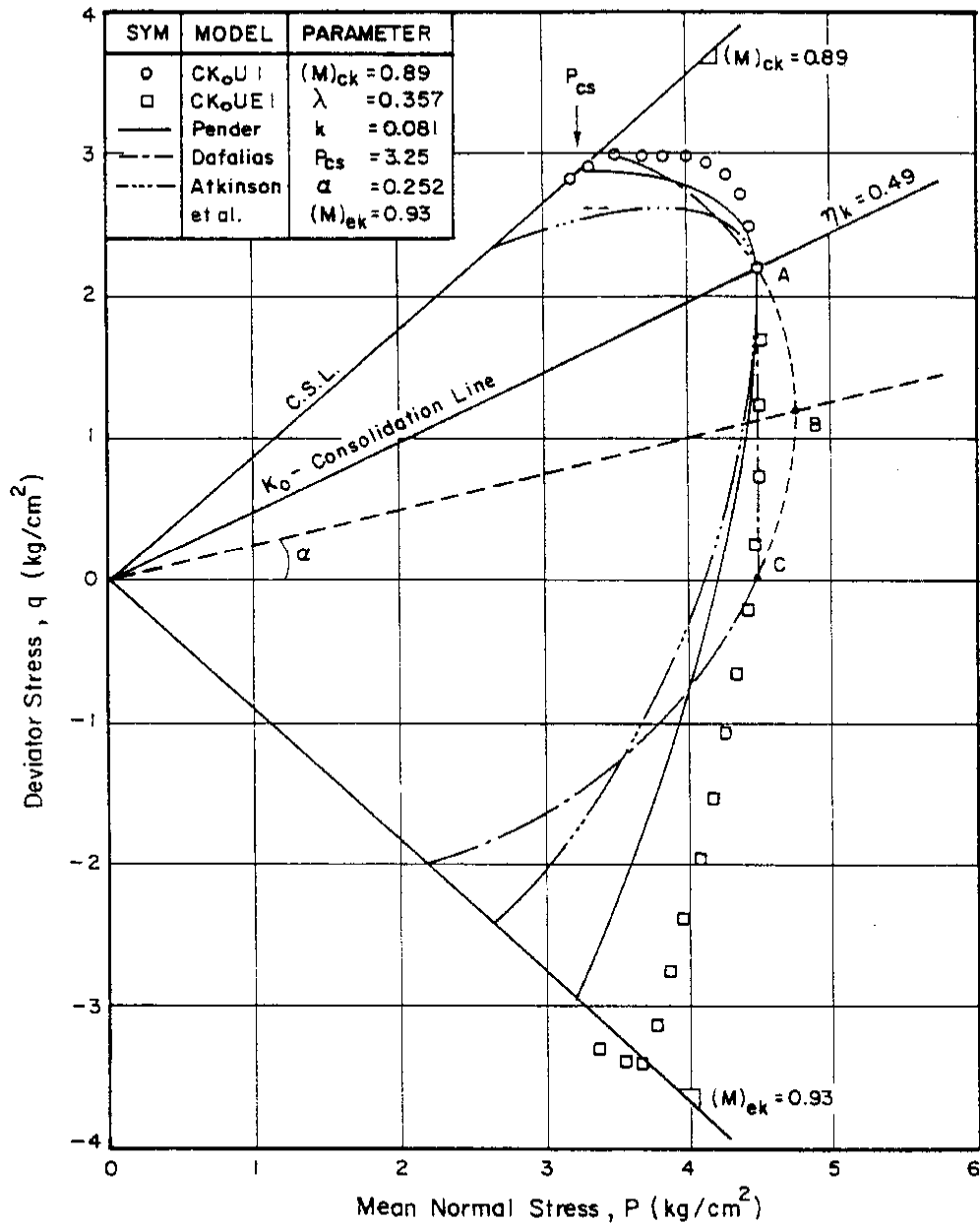


**Fig. 5 ( $q/p$ ) Plot for  $K_0$ -normally Consolidated Samples Compared with Predictions from Pender's Model (Critical State)**

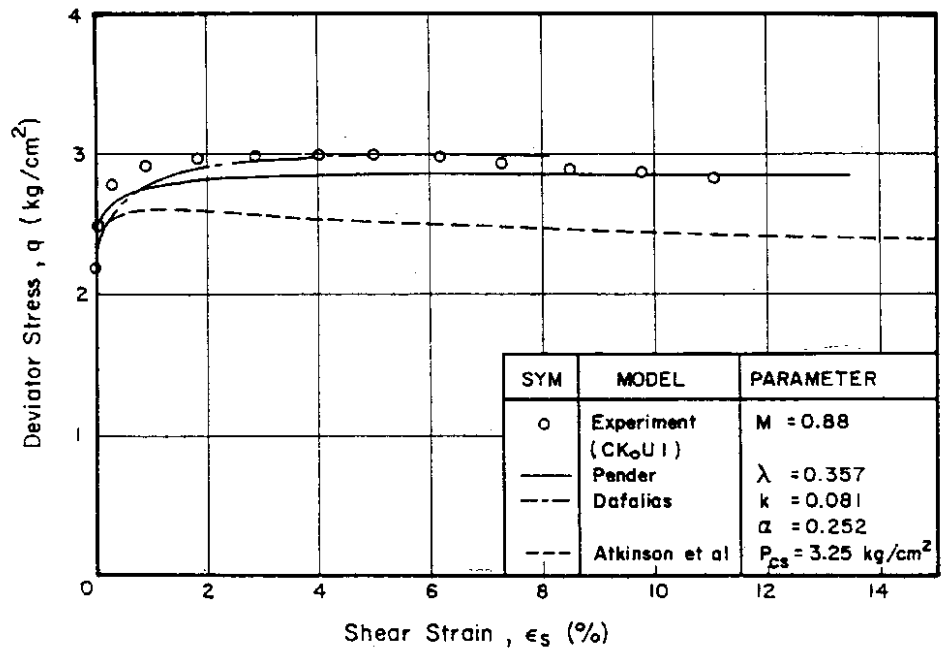


Fig. 6a ( $q/\epsilon_s$ ) Plot for CK<sub>0</sub>U1 Sample Compared with the Model Predictions in Compression Conditions

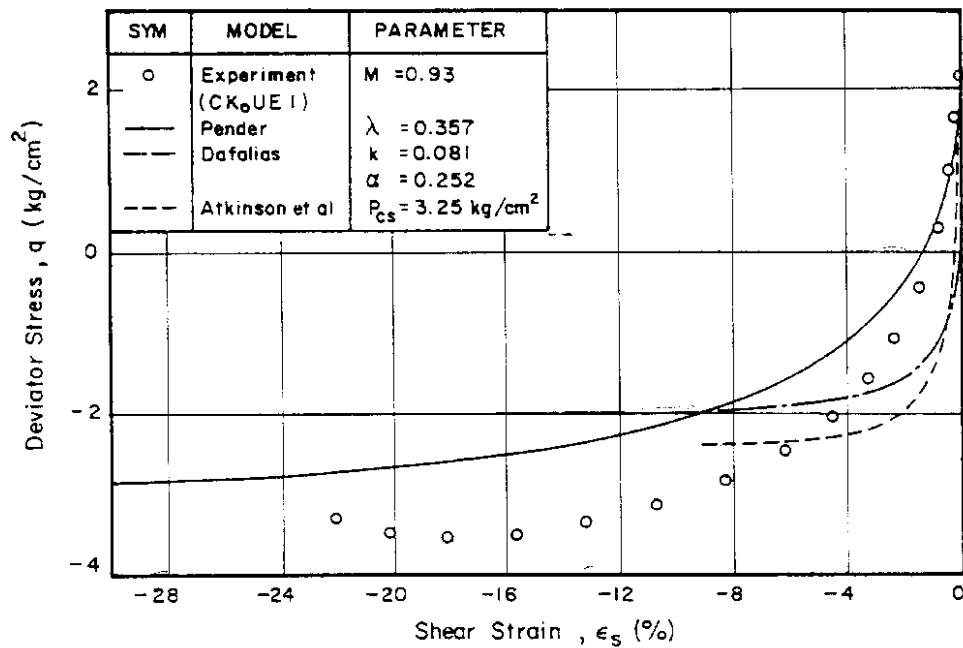
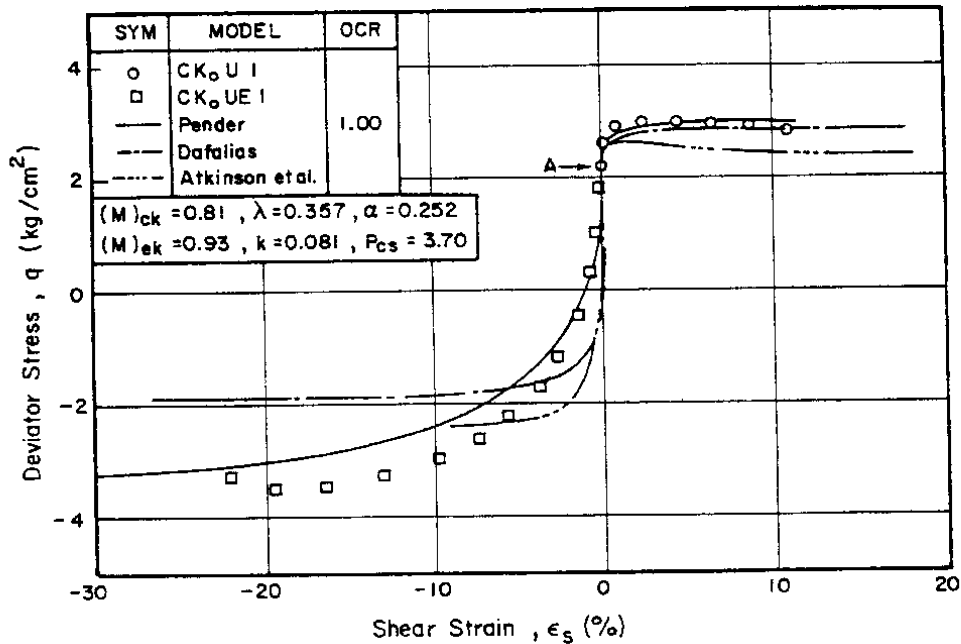


Fig. 6b ( $q/\epsilon_s$ ) Plot for CK<sub>0</sub>UE1 Sample Compared with the Model Predictions in Compression Conditions



## CRITICAL STATE MODELS



**Fig. 7 ( $q/\epsilon_s$ ) Plot for  $K_0$ -normally Consolidated Samples Compared with the Model Predictions (Peak Stress State)**

### Excess Pore Pressure

Figures 8 and 9 present the excess pore pressure versus shear strain relationships. All models predict roughly the same  $(u, \epsilon_s)$  relationship up to a shear strain of about 3% in the compression phase. Thereafter, they deviate from each other with increasing shear strains. All models tend to overpredict the excess pore pressures.

The patterns of model prediction in the extension phase are quite different from those in compression. Pender's Model gives a trend similar to the experimental data, although it underpredicts the negative pore pressures. This tendency is improved when the parameters are determined from the peak deviator stress condition. On the other hand, Dafalias' and Atkinson's Models predict positive pore pressures when the strain exceeds about 2%.

### Variation of Parameter $\alpha$ in Dafalias' Model (1987)

The magnitude of  $\alpha$  determines the shape of the volumetric yield locus and the undrained stress path for the  $K_0$ -consolidated clays. However, it is not a necessary condition that  $\alpha$  should remain constant during the subsequent shear.

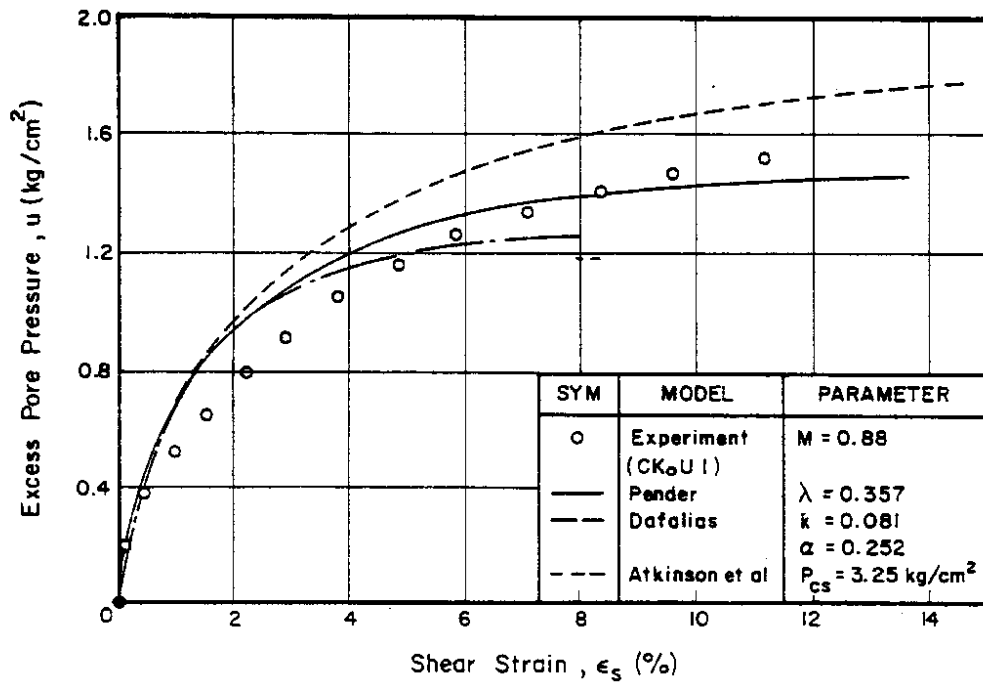


Fig. 8 ( $u/\epsilon_s$ ) Plot for CK<sub>o</sub>U1 Sample Compared with the Model Predictions

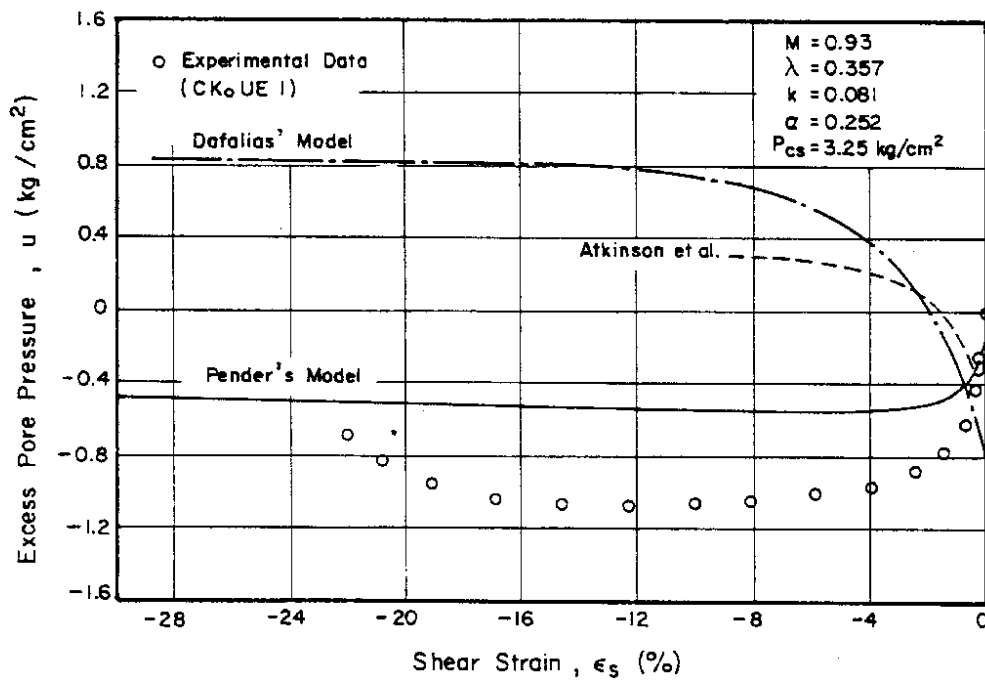
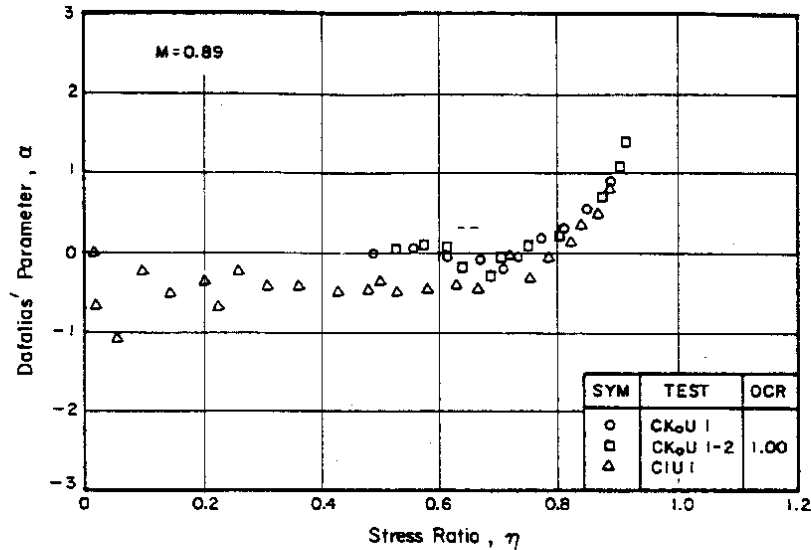


Fig. 9 ( $u/\epsilon_s$ ) Plot for CK<sub>o</sub>UE1 Sample Compared with the Model Predictions

## CRITICAL STATE MODELS

The  $\alpha$  values are plotted with respect to the stress ratio in Fig. 10. The  $\alpha$  values for the  $K_o$ -normally consolidated samples remain constant up to a stress ratio of about 0.7, thereafter, it increases rapidly as the stress ratio is increased. The variation of  $\alpha$  values with stress ratio for the  $K_o$ -overconsolidated samples during the undrained compression tests are plotted in Fig 11. It can be concluded from these figures that the value of  $\alpha$  varies during shear.



**Fig. 10 Variations of Dafalias'  $\alpha$ -parameter with the Stress Ratio for  $K_o$ -normally Consolidated Samples**

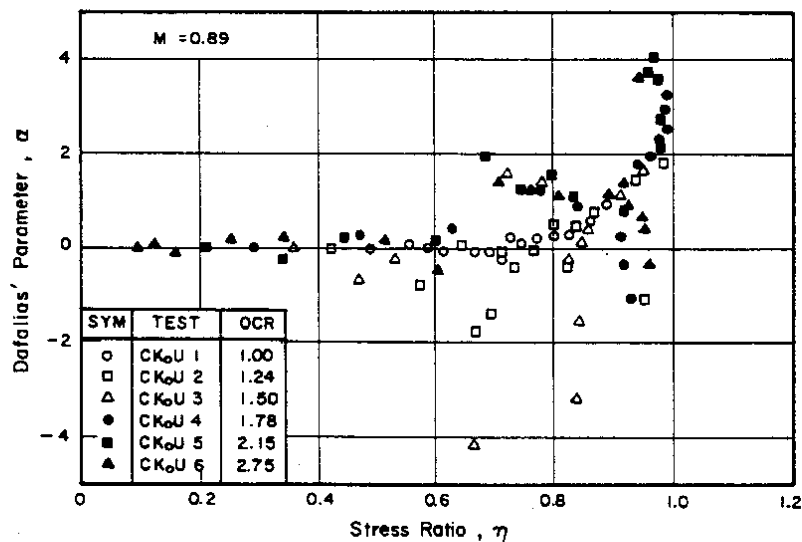


**Fig. 11 Variations of Dafalias'  $\alpha$ -parameter with the Stress Ratio for  $K_o$ -overconsolidated Samples**

# COMPARISON OF UNDRAINED BEHAVIOR OF OVERCONSOLIDATED SAMPLE SHEARED FROM $K_0$ PRE-SHEAR STRESS CONDITIONS

In this section, Pender's Model on overconsolidated undrained behavior is examined both in compression and in extension.

## Triaxial Compression

1. **Undrained Stress Paths** - The undrained stress paths predicted by Pender's Model for the  $K_0$ -overconsolidated samples are superimposed With the test data in Fig. 12. Model parameters used for the calculations are determined from the Critical State condition. The deviations are pronounced as the overconsolidation ratio is increased.

2. **Stress-Strain Relationships** - The stress-strain relationships are compared with test data in Fig. 13. Pender's Model overpredicts the strain. This trend becomes pronounced as the overconsolidation ratio is increased.

3. **Excess Pore Pressure-Strain Relationships** - Figure 14 shows the pore pressure-shear strain relationships. The figure indicates that the Pender's Model underpredicts the excess pore pressure at certain levels of shear strains. The deviations are particularly substantial for the samples sheared from the dry side of the Critical State. This may indicate that the assumption made on the plastic strain increment ratio in the theory is not realistic.

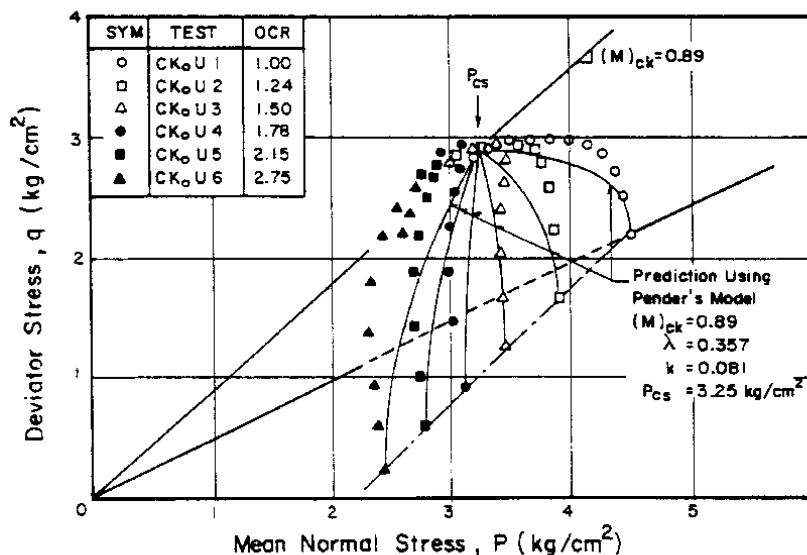
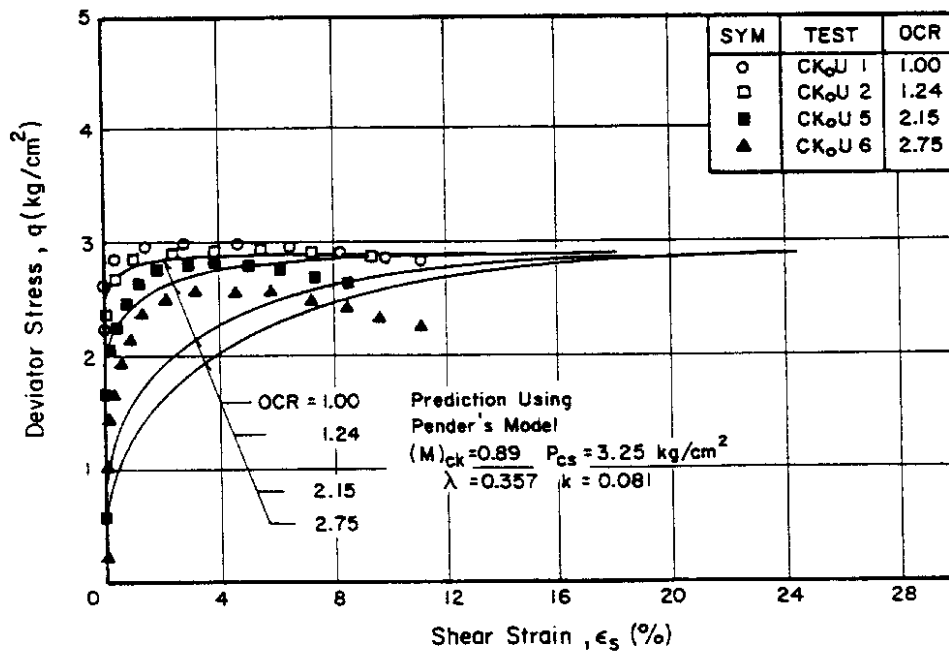
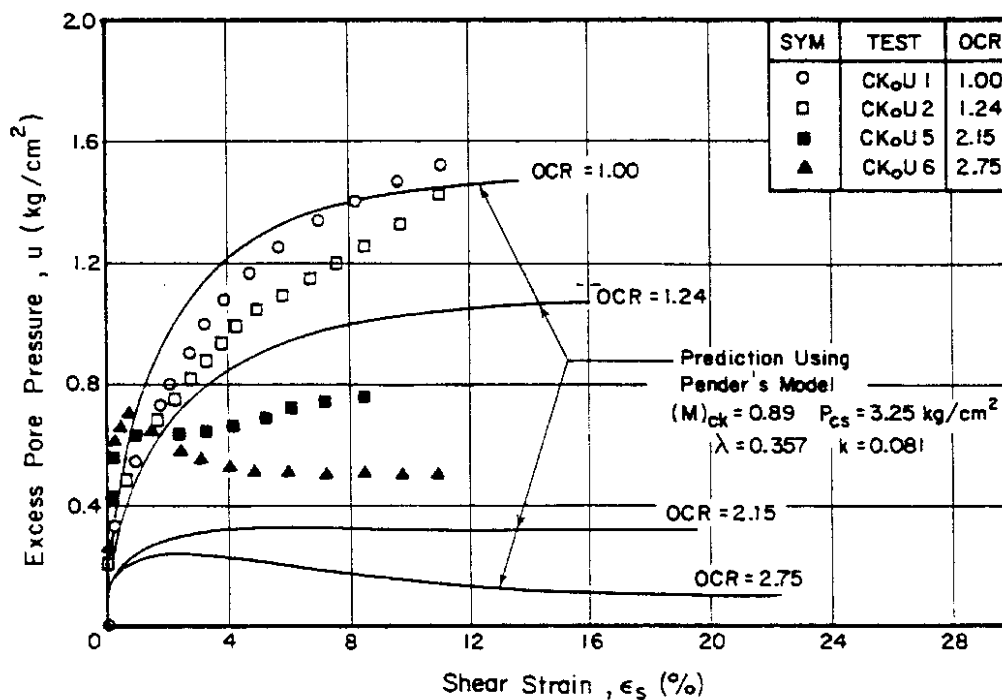


Fig. 12  $(q, p)$  Plot for  $K_0$ -overconsolidated Samples Compared with the Predictions from Pender's Model (Critical State)

# CRITICAL STATE MODELS



**Fig. 13 ( $q, \epsilon_s$ ) Plot for  $K_o$ -overconsolidated Samples Compared with the Predictions from Pender's Model (Critical State)**



**Fig. 14 ( $u, \epsilon_s$ ) Plot for  $K_o$ -overconsolidated Samples Compared with the Predictions from Pender's Model (Critical State)**

### Triaxial Extension

1. **Undrained Stress Paths** - Figure 15 displays the undrained stress paths in the extension tests together with those in the compression tests. The parameters used in the predictions are determined from the peak deviator stress condition. The model predictions for the extension conditions is better than those for the compression conditions, especially, for the samples sheared from the dry side of the Critical State.

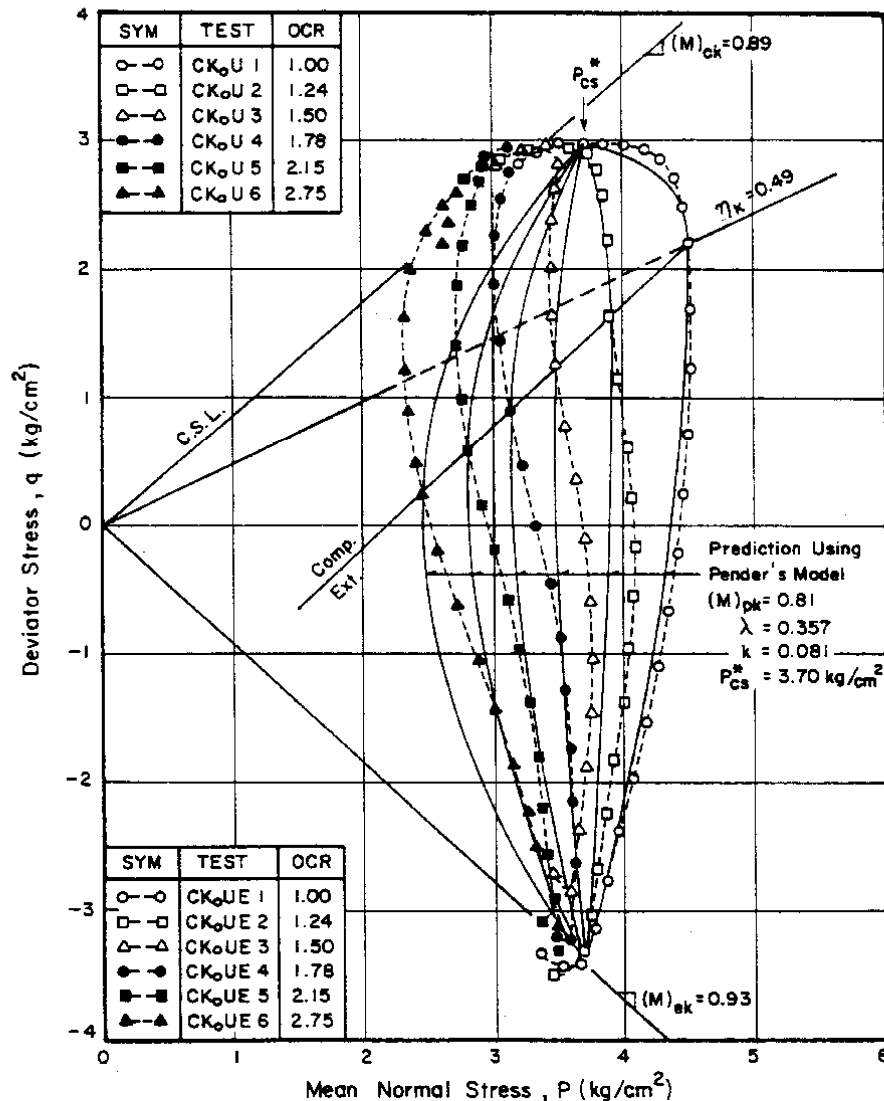


**Fig. 15**  $(q, p)$  Plot for  $K_0$ -overconsolidated Samples both in Compression and in Extension Conditions Compared with the Predictions from Pender's Model (Peak Stress State)

## CRITICAL STATE MODELS

2. **Stress-Strain Relationships** - The stress-strain relationships for the extension conditions are compared in Fig. 16. The model predicts the stress-strain relationships well.

3. **Excess Pore Pressure-Strain Relationships** - The relationship between the excess pore pressure and the shear strains are shown in Fig. 17. The Model predicts successfully the excess pore pressure for the normally consolidated sample in the extension condition. However, the predictions are not good for the overconsolidated samples.

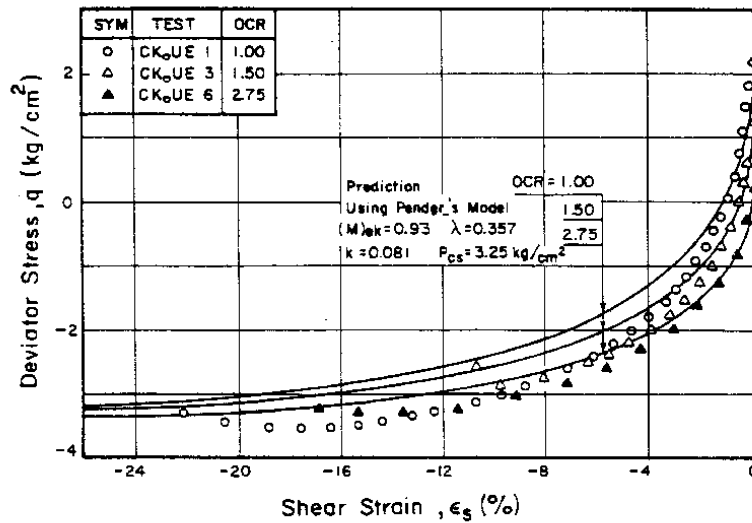


**Fig. 16 ( $q, \epsilon_s$ ) Plot for  $K_o$ -overconsolidated Samples in Extension Conditions Compared with the Predictions from Pender's Model**

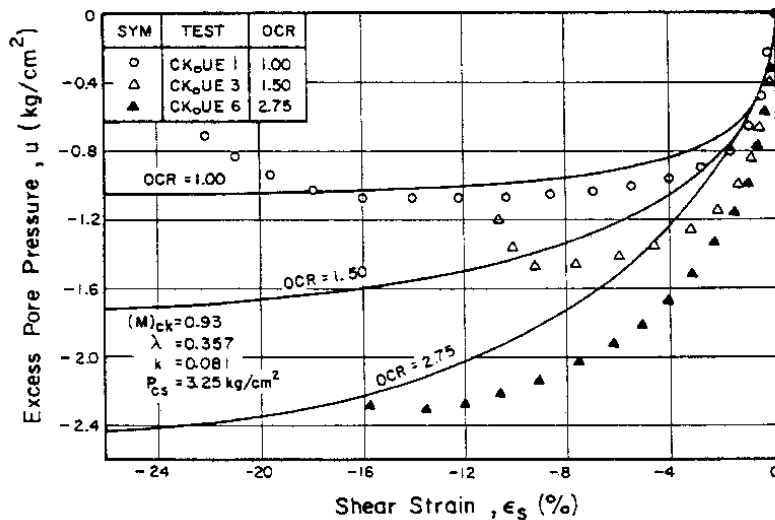


**Fig. 17 ( $u, \epsilon_s$ ) Plot for  $K_o$ -overconsolidated Samples in Extension Conditions Compared with the Predictions from Pender's Model**

## **COMPARISON OF DRAINED BEHAVIOR OF NORMALLY CONSOLIDATED CLAYS SHEARED FROM $K_o$ PRE-SHEAR STRESS CONDITIONS**

Drained test data from  $K_o$ -normally consolidated samples are compared with model predictions. The models used in the comparisons are Pender's Model (Pender, 1977, 1978), Dafalias' Model (Dafalias, 1987) and Atkinson's Model (Atkinson, et al., 1987).

### **Triaxial Compression**

1. **Stress-Strain Relationships** - Figures 18 and 19 show the  $(q, \epsilon_s)$  and  $(q, \epsilon_v)$  relationships for the  $CK_oD1$  specimen, respectively. The prediction of shear strain from all the models is good up to deviator stress of  $3.2 \text{ kg/cm}^2$ . During further increase in deviator stress, the predictions using Pender's and Atkinson's Models deviated from the test data, while those using Dafalias' Model are surprisingly close to the experimental observations. Dafalias' Model also gives an excellent prediction of volumetric strains, while the other two models overpredict the volumetric strains.

2. **Plastic Volumetric Strain-Plastic Shear Strain Relationships** - Figure 20 illustrates the  $(\epsilon_{vp}, \epsilon_s)$  relationship for the  $K_o$ -normally consolidated sample ( $CK_oD1$  sample) during the conventional loading test. The prediction using Dafalias' Model agrees well with the test data. Pender's Model predicts smaller plastic volumetric strains, while Atkinson's Model predicts larger ones at the same level of shear strain.

### **Triaxial Extension**

The behavior of normally consolidated sample becomes overconsolidated immediately after applying the conventional type of unloading. Therefore,  $CK_oDE1$  state paths no longer lie on the State Boundary Surface (SBS). Only Pender's Model is applicable for predictions under this condition, since it deals with the overconsolidated behavior.

**Stress-Strain Relationships** - The comparisons of  $(q, \epsilon_s)$  relationships between test data and model predictions during the conventional drained unloading test on  $K_o$ -normally consolidated samples are shown in Fig. 21. Pender's model makes an excellent prediction during unloading in compression. The predictions for the stress states below the  $p$ -axis begin to deviate from the test data. The other two models give smaller strain than the test data up to the deviator stress close to failure.



## CRITICAL STATE MODELS

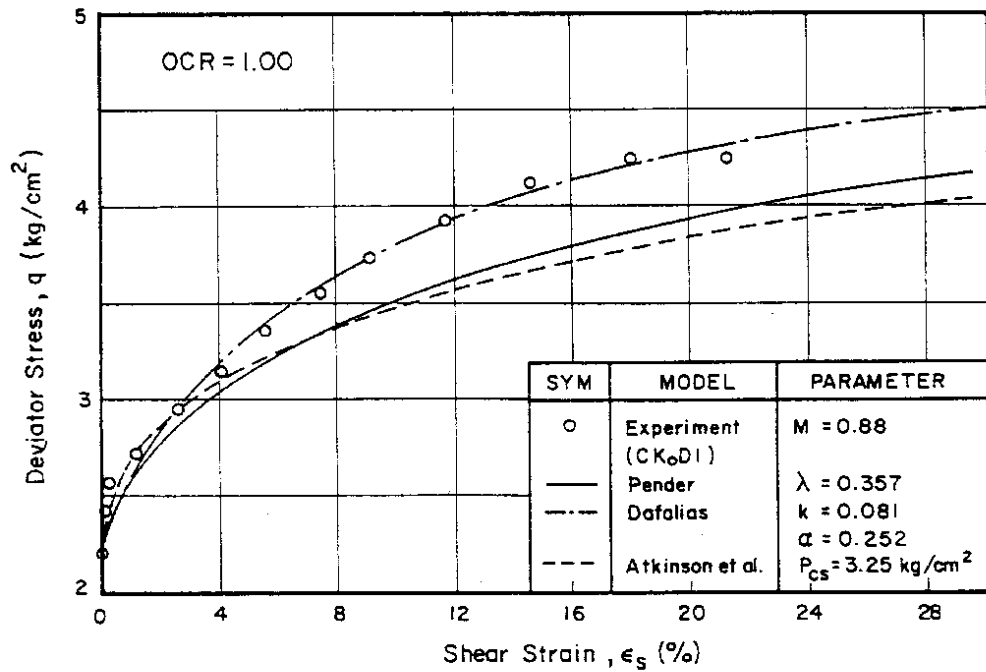


**Fig. 18 ( $q, \epsilon_s$ ) Plot for CK<sub>1</sub> Sample Compared with the Model Predictions**

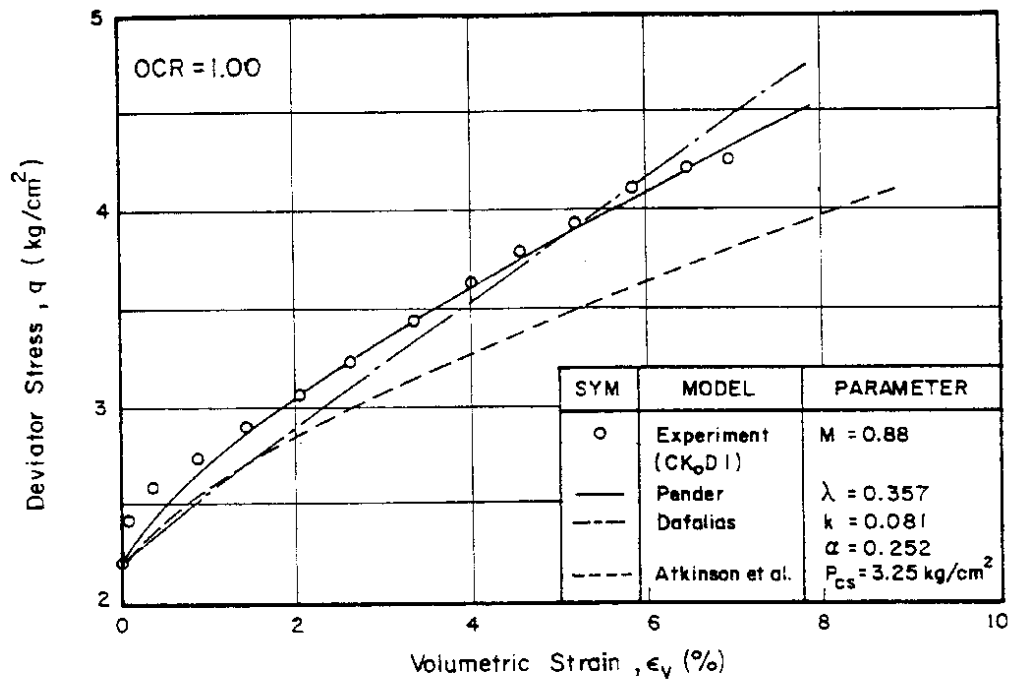


**Fig. 19 ( $q, \epsilon_v$ ) Plot for CK<sub>1</sub> Sample Compared with the Model Predictions**

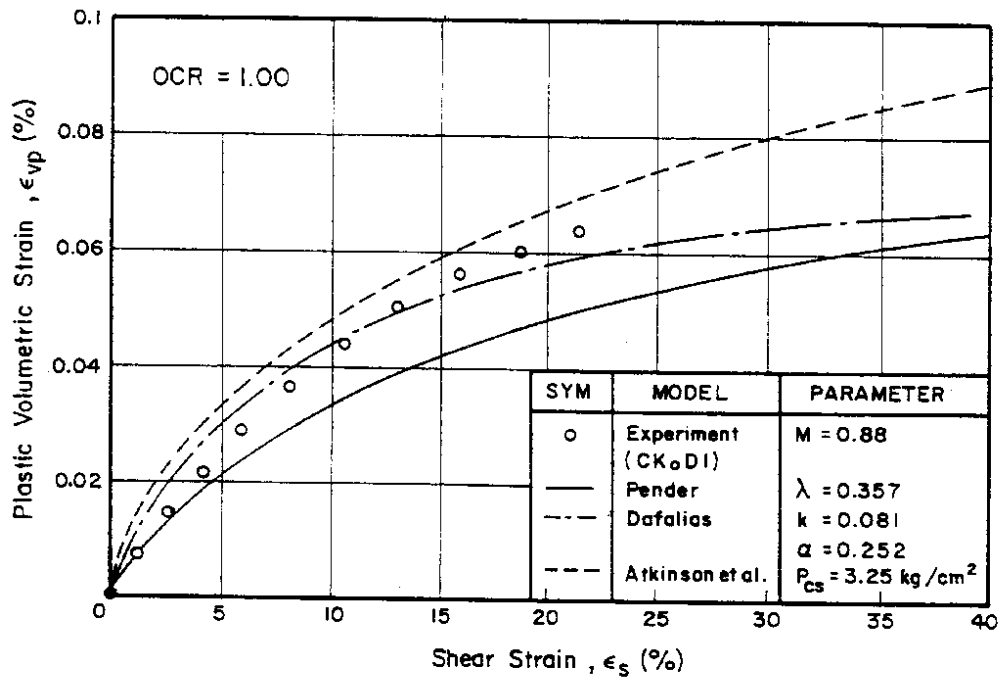


Fig. 20 ( $\epsilon_{vp}$ ,  $\epsilon_s$ ) Plot for CK<sub>o</sub>1 Sample Compared with the Model Predictions

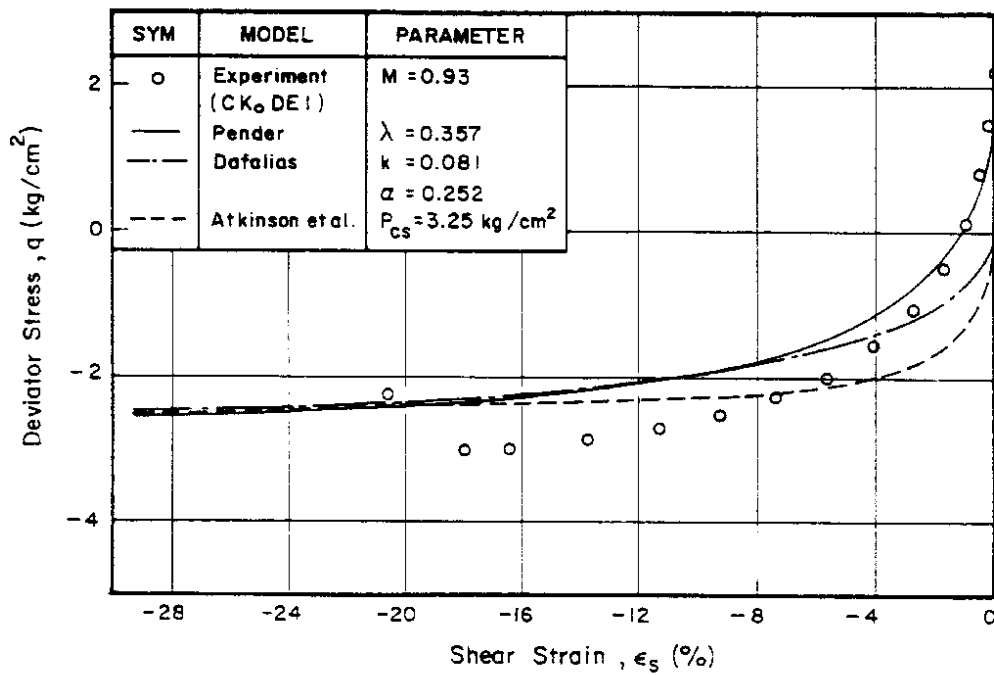


Fig. 21 ( $q$ ,  $\epsilon_s$ ) Plot for CK<sub>o</sub>DE1 Sample Compared with the Model Predictions

## CRITICAL STATE MODELS

### COMPARISON OF DRAINED BEHAVIOR OF OVERCONSOLIDATED CLAYS SHEARED FROM $K_o$ PRE-SHEAR STRESS CONDITIONS

The behavior from a total of six series of drained tests on  $K_o$ -overconsolidated samples are compared with the predictions using Pender's Model (Pender, 1978).

#### Conventional Drained Compression Tests ( $CK_oD$ Tests)

**Stress-Strain Relationships** - Figures 22 and 23 illustrate the stress-strain relationships for  $CK_oD$  tests. Pender's Models overpredict shear strain (Fig. 23). The deviations increased with the increase in OCR values. In the case of the deviator stress-volumetric strain relationship demonstrated in Fig. 23, the prediction is improved except for the sample sheared from the dry side of the Critical State ( $CK_oD6$ ).

#### Constant $p$ Compression Tests ( $CK_oPC$ Tests)

**Stress-Strain Relationships** - Figures 24 and 25 present the  $(q, \epsilon_s)$  and the  $(q, \epsilon_v)$  relationships predicted using Pender's Model together with the corresponding test data. The model predictions agree well with test data from  $CK_oPC1$  and  $CK_oPC2$  specimens. On the other hand, larger shear strains for the sample with higher OCR values at the same level of deviator stress are given (see  $CK_oPC4$  and  $CK_oPC6$  samples). Deviations especially begin to occur from a very early stage of shearing. A similar contrast for the  $(q, \epsilon_v)$  relationships is also seen in Fig. 25. This again indicates that Pender's Model can provide good predictions of volumetric strain for overconsolidated samples.

#### Unloading Compression Test ( $CK_oDU$ Test)

**Stress-Strain Relationships** - All the stress states for these overconsolidated samples lie within the State Boundary Surface. Figures 26 and 27 illustrate the  $(q, \epsilon_s)$  and  $(q, \epsilon_v)$  relationships, respectively. The predictions deviate substantially from the observed behavior when the OCR values increased. Pender's Model overpredicts shear strain for the overconsolidated samples. However, the predictions for the sample with a OCR value of 1.24 agree well with the observations. Figure 27 provides further evidence that Pender's Model can successfully predict volumetric strains for overconsolidated specimens.

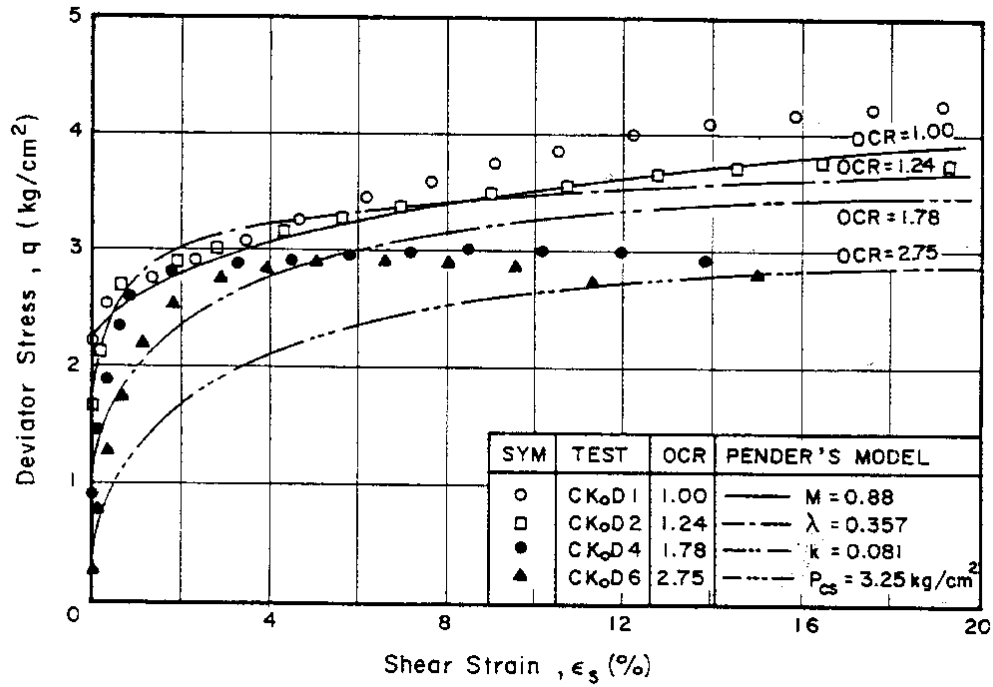


Fig. 22 ( $q, \epsilon_s$ ) Plot for CK<sub>o</sub>D Samples Compared with the Model Predictions

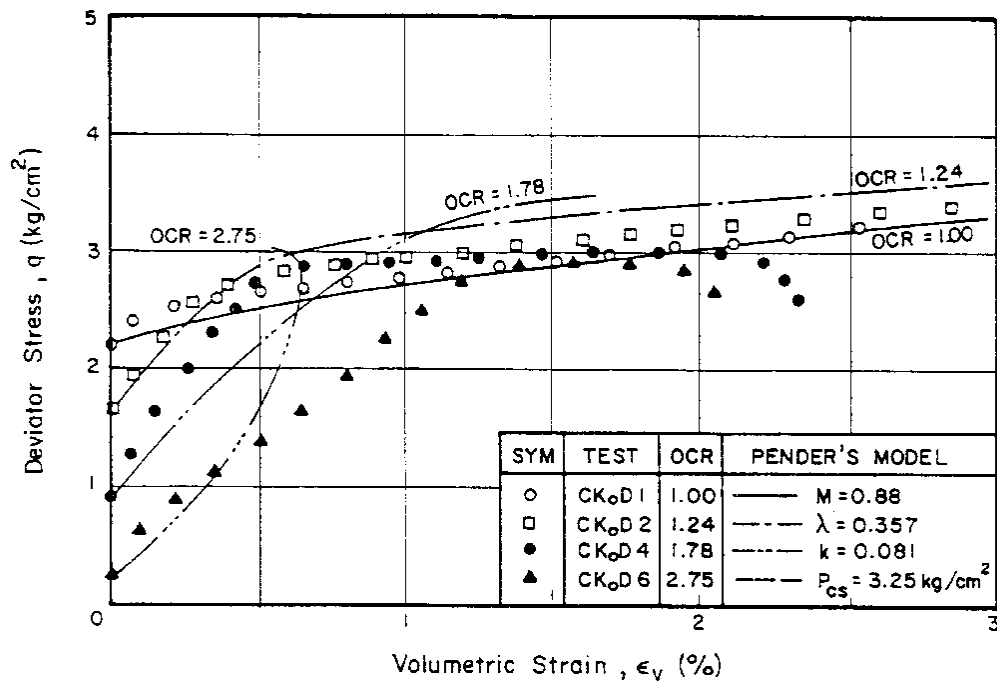
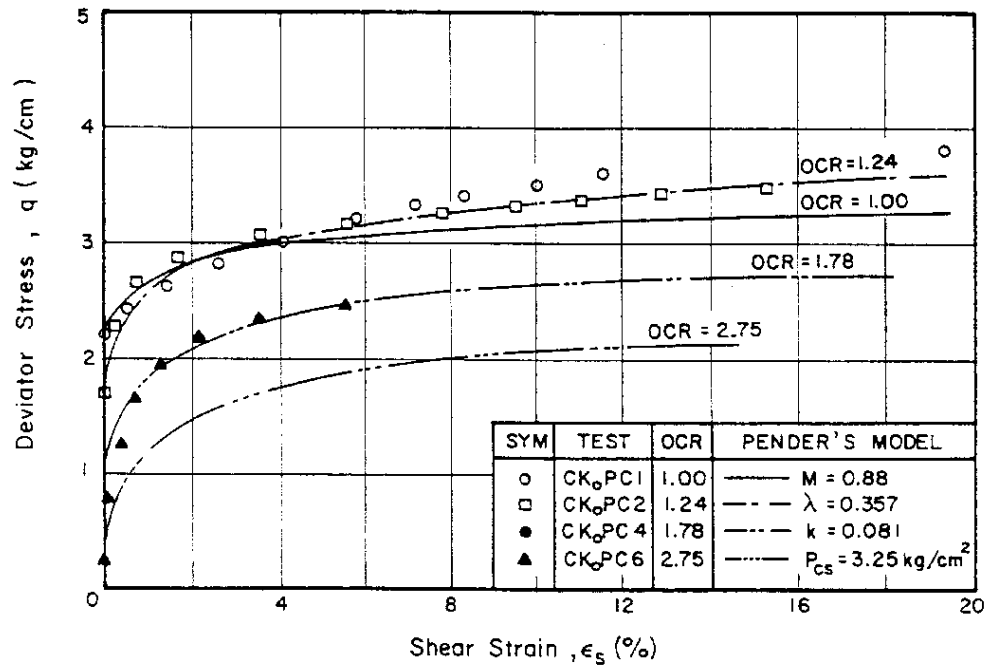
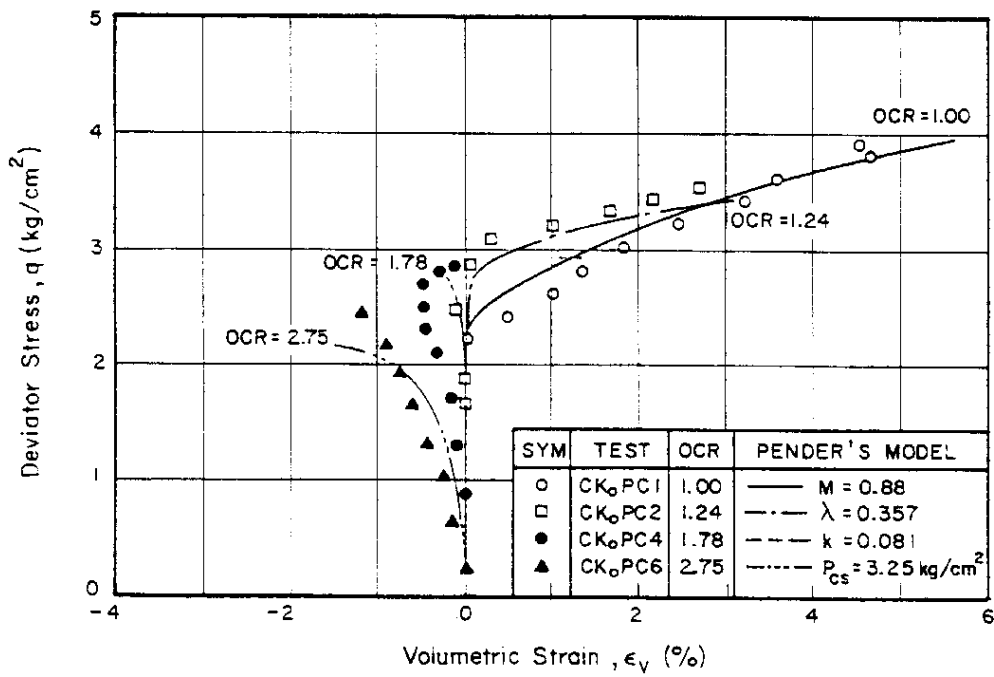


Fig. 23 ( $q, \epsilon_v$ ) Plot for CK<sub>o</sub>D Samples Compared with the Model Predictions

## CRITICAL STATE MODELS



**Fig. 24 ( $q, \epsilon_s$ ) Plot for CK<sub>o</sub>PC Samples Compared with the Model Predictions**



**Fig. 25 ( $q, \epsilon_v$ ) Plot for CK<sub>o</sub>PC Samples Compared with the Model Predictions**

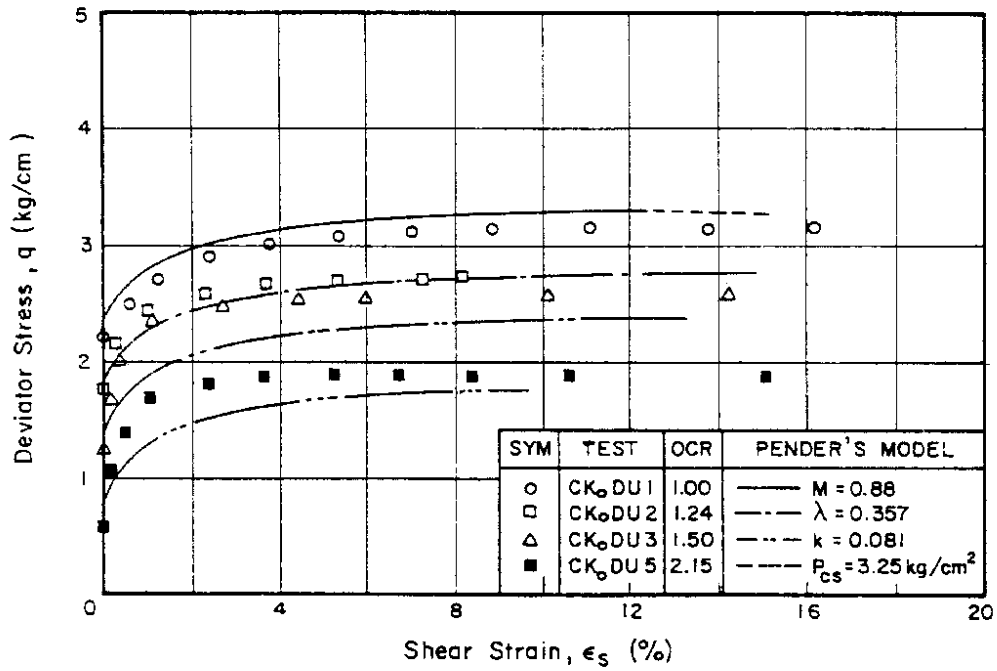


Fig. 26 ( $q, \epsilon_s$ ) Plot for CK<sub>o</sub>DU Samples Compared with the Model Predictions

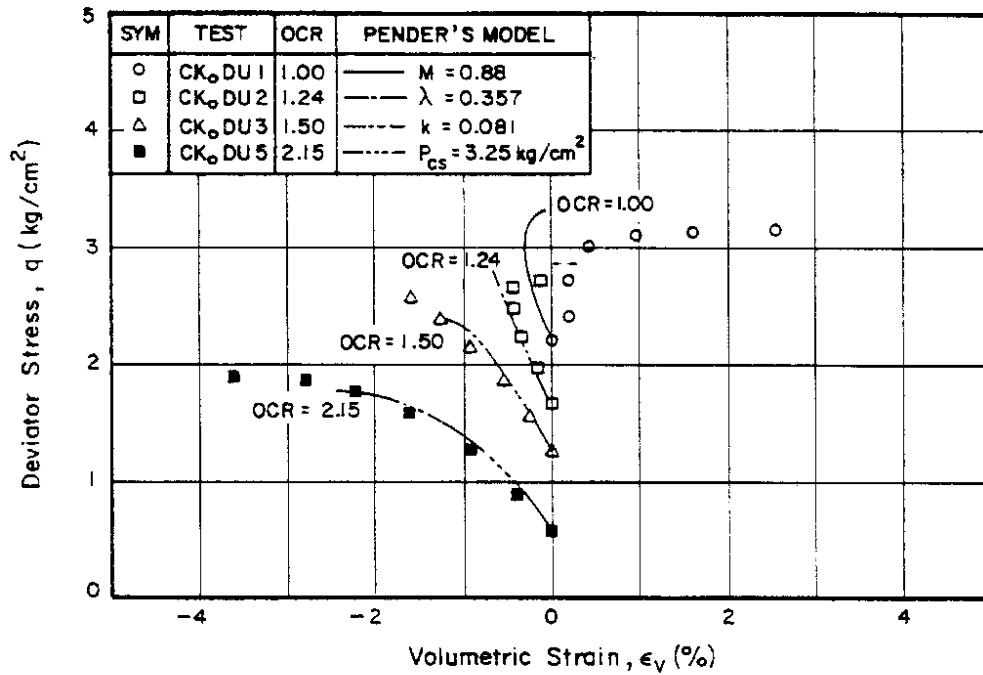


Fig. 27 ( $q, \epsilon_v$ ) Plot for CK<sub>o</sub>DU Samples Compared with the Model Predictions

## CRITICAL STATE MODELS

### Constant $q$ Unloading Tests ( $CK_oQU$ Tests)

All the state paths of the samples belonging to this test series lie within the State Boundary Surface. The  $M$  values used for the calculations are 1.16, 1.18, 1.28 and 1.48 corresponding to samples  $CK_oQU1$ ,  $CK_oQU2$ ,  $CK_oQU3$  and  $CK_oQU5$ , respectively.

**Stress-Strain Relationships** - Figure 28 contains the  $(\varepsilon_v, p)$  relationships of the  $CK_oQU$  test series compared with the predictions. The predictions for volumetric strains agree well with the experimental observations.

### Conventional Drained Extension Tests ( $CK_oDE$ Tests)

All the state paths of these samples lie within the State Boundary Surface.

**Stress-Strain Relationships** - Figures 29 and 30 display  $(q, \varepsilon_s)$  and  $(q, \varepsilon_v)$  relationships, respectively. The shear strains predicted agree well with test data up to a deviator stress of  $-1.0 \text{ kg/cm}^2$ . Below this deviator stress level, the predicted shear strains are larger for the  $CK_oDE1$  and  $CK_oDE2$  samples. For the  $CK_oDE4$  and  $CK_oDE5$  samples, the predictions agree well with the test data. Unlike the case of the compression tests, the predictions of the volumetric strain for the extension tests deviate as shown in Fig. 30. However, the predictions are acceptable for a first order approximation.

### Constant $p$ Extension Tests ( $CK_oPE$ Tests)

**Stress-Strain Relationships** - Figures 31 and 32 demonstrate the variations of the shear strain and the volumetric strains with respect to the deviator stress. The predictions are better for the samples with higher OCR values. This indicates that Pender's Model overpredicts shear strain as the initial state of the sample is close to the normally consolidated state. In the case of overconsolidated samples, the predicted shear strains are larger probably after the yielding took place. The  $(q, \varepsilon_v)$  relation predicted using Pender's Model deviates from all the actual observations as shown in Fig. 32.

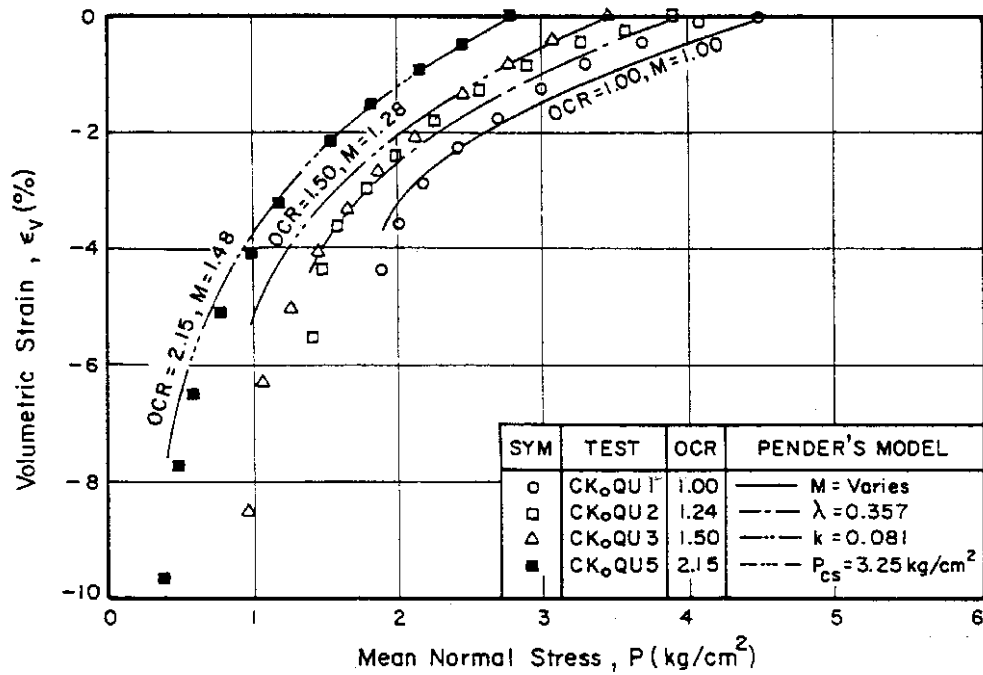


Fig. 28 ( $\epsilon_v, p$ ) Plot for CK<sub>o</sub>QU Samples Compared with the Model Predictions

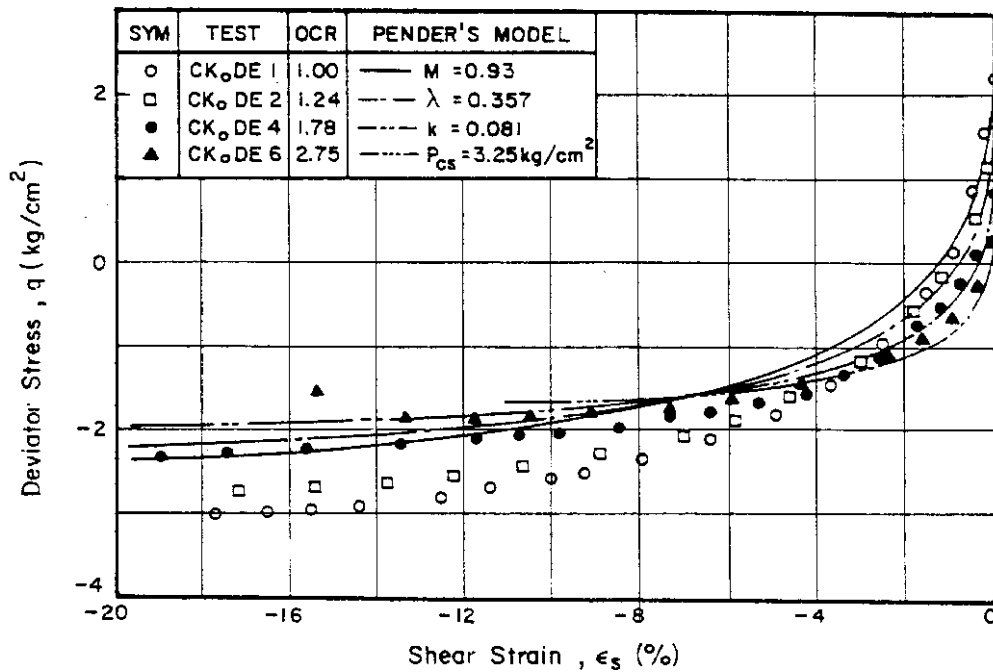
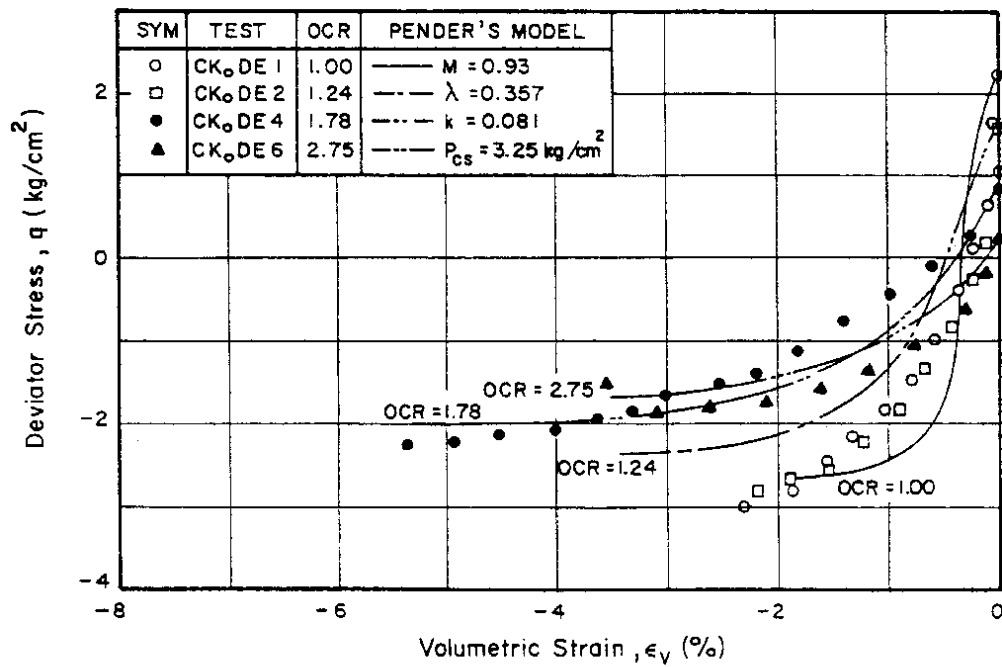


Fig. 29 ( $q, \epsilon_s$ ) Plot for CK<sub>o</sub>DE Samples Compared with the Model Predictions



## CRITICAL STATE MODELS



**Fig. 30 ( $q, \epsilon_v$ ) Plot for CK<sub>o</sub>DE Samples Compared with the Model Predictions**

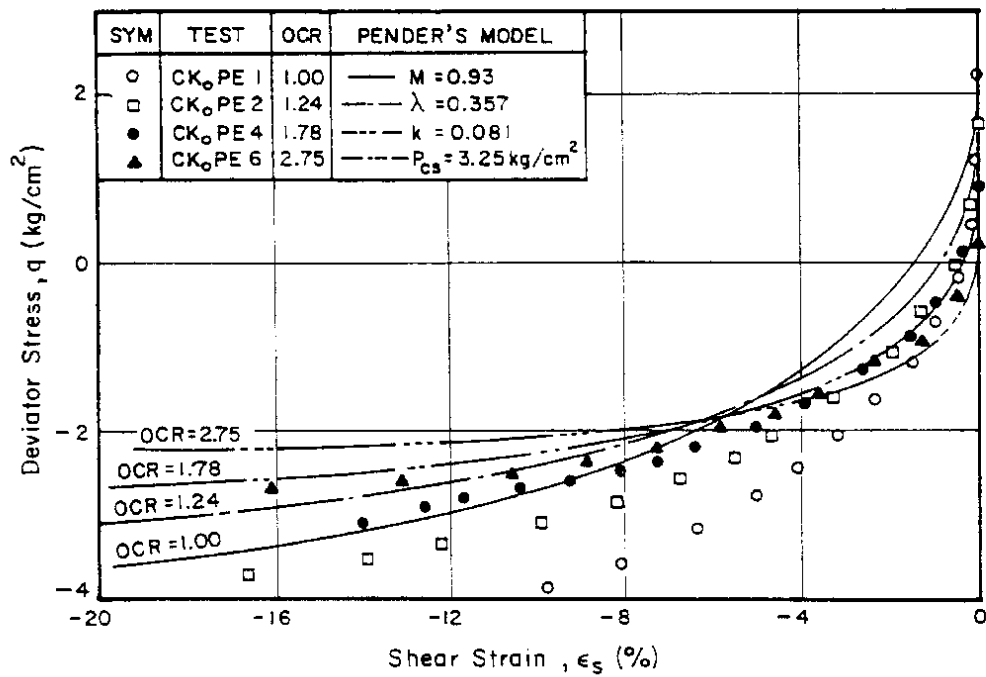


**Fig. 31 ( $q, \epsilon_s$ ) Plot for CK<sub>o</sub>PE Samples Compared with the Model Predictions**

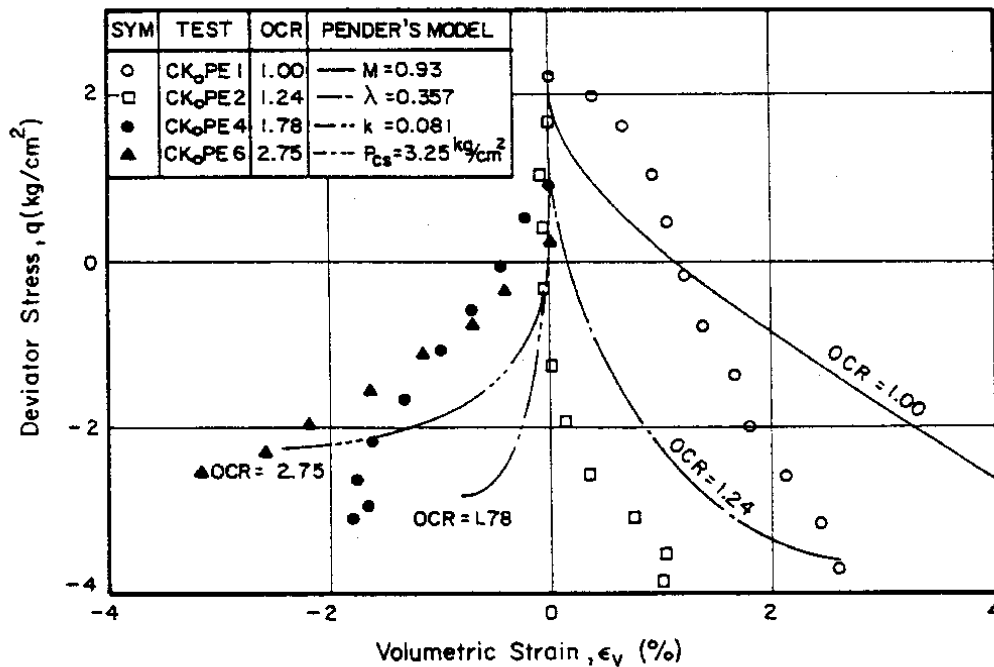


Fig. 32 ( $q, \epsilon_v$ ) Plot for CK<sub>o</sub>PE Samples Compared with the Model Predictions

### A CONCEPTUAL MODIFICATION OF PENDER'S MODEL FOR THE $K_o$ -OVERCONSOLIDATED SAMPLES

#### Undrained Stress Paths

The behavior of the  $K_o$ -overconsolidated samples in the compression conditions is rigid nearly up to the failure state. A typical illustration of the rigid behavior is the vertical rise-up of the undrained stress path for almost the full range of the deviator stress. This implied that the behavior of the overconsolidated clay can be treated as pseudo-elastic at least up to a deviator stress equal to the initial deviator stress in the normally consolidated state as imposed during the sample preparation. The strain prediction will be more realistic, if Pender's Model is applied only for deviator stresses higher than the initial values imposed on the samples during the sample preparation. Figure 33 illustrates the undrained stress paths as proposed above in a modified form of prediction and the actual prediction using Pender's Model. Line OB is the base line for Pender's Model, i.e., the initial stress points of the overconsolidated sample are all shifted to this horizontal line. The region between the line OA and OB is considered as a pseudo-elastic zone. The proposed undrained stress paths appear to be promising as indicated in Fig. 34. The prediction of the undrained paths are much improved.

## CRITICAL STATE MODELS

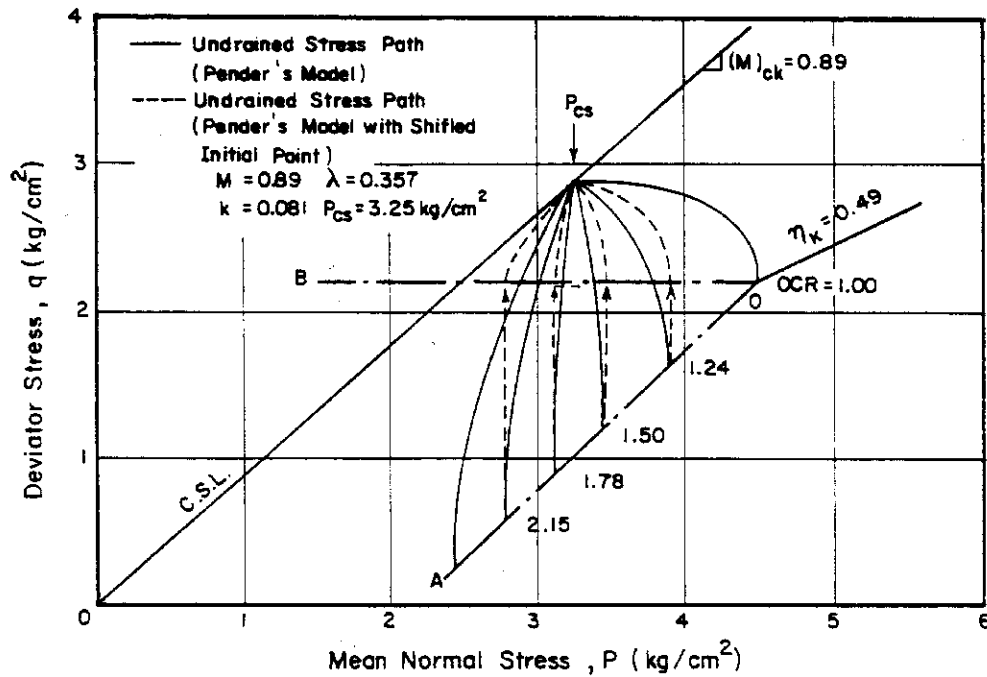


**Fig. 33  $(q, p)$  Plot from Pender's Model with and without Shifted Initial Stress Points**

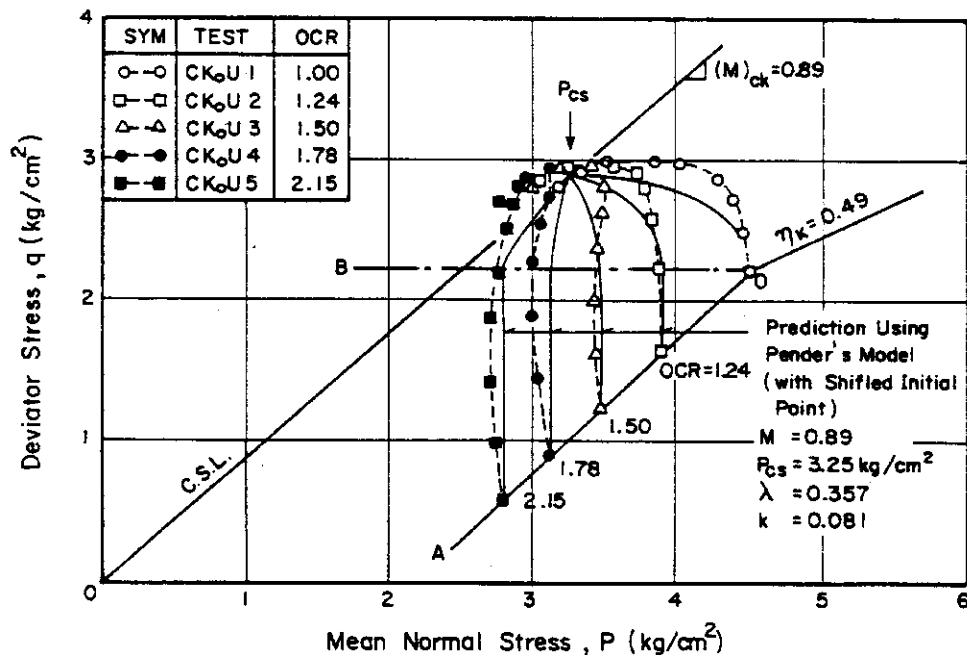


**Fig. 34  $(q, p)$  Plot for  $K_o$ -overconsolidated Samples Compared with the Predictions from Pender's Model with Shifted Initial Stress Points**

### **Stress-Strain and Pore Pressure-Strain Relationships**

Stress-strain relationships from Pender's Model as used in a modified form are plotted together with the experimental data in Fig. 35 (wet zone) and Fig. 36 (dry zone), respectively. These figures demonstrate that the proposed modified approach drastically improve the predicted stress-strain relationships. The same trends are shown in Figs. 37 and 38 for the pore pressure-strain relationships.

### **CONCLUDING REMARKS AND COMMENTS OF THE MODEL EVALUATION**

The stress-strain theories based on the Critical State Concepts are examined by comparing the predictions with the experimental observations. For the  $K_o$ -consolidated samples, all model predictions deviate from the experimental observations, particularly, they fail to simulate the undrained stress path in the early stages of loading. Furthermore, all models are poor in their predictions of the  $K_o$  extension behavior. Brief concluding remarks for each model are made below.

#### **Undrained Behavior of Normally Consolidated Samples**

1. **Pender's Model** - For the  $CK_oU$  test, Pender's Model predicts reasonably well the undrained stress paths both in compression and in extension with parameters determined from the peak deviator stress criterion. However, it overpredicts shear strains in the compression phase, and gives poor strain predictions in extension.
2. **Dafalias' Model** - This model provides good stress-strain predictions for the compression tests. However, its prediction for the extension tests is poor, especially at the larger strains. The parameter  $\alpha$  varies during undrained shearing and is not zero even for the isotropically consolidated sample whereas it should be according to the theory.
3. **Atkinson et al.'s Model** - Atkinson's Model predicts low undrained strength in compression, and its predictions for the extension conditions are poor specifically for the larger strain range.

#### **Undrained Behavior of Overconsolidated Samples**

**Pender's Model** - Pender's Model generates a successful family of undrained stress paths for the overconsolidated clays on the wet side of the Critical State both for compression and for extension conditions when the parameters are selected from the

## CRITICAL STATE MODELS

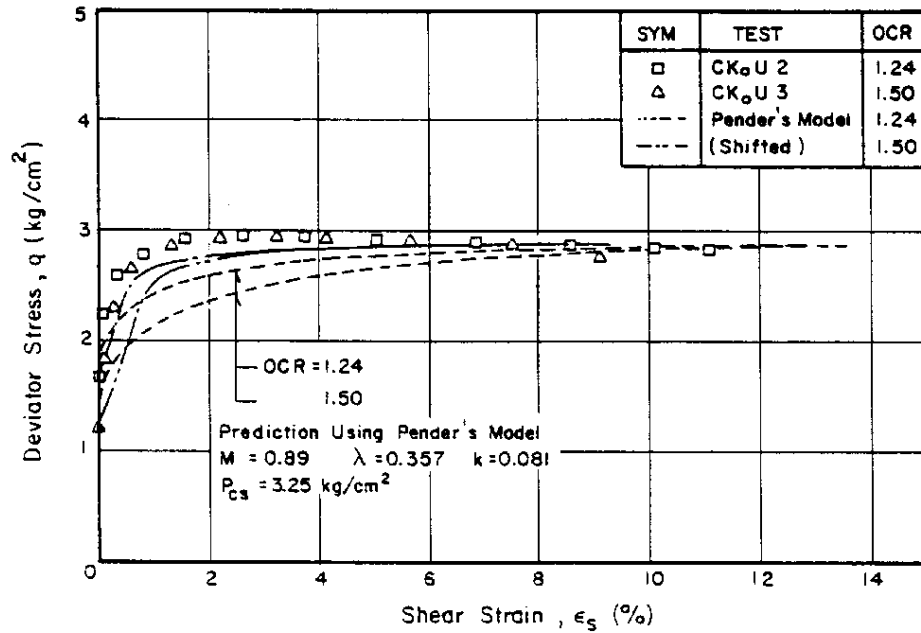


**Fig. 35 ( $q, \epsilon_s$ ) Plot for  $K_0$ -overconsolidated Samples Compared with the Predictions from Pender's Model with and without Shifted Initial Stress Points (Wet Zone)**

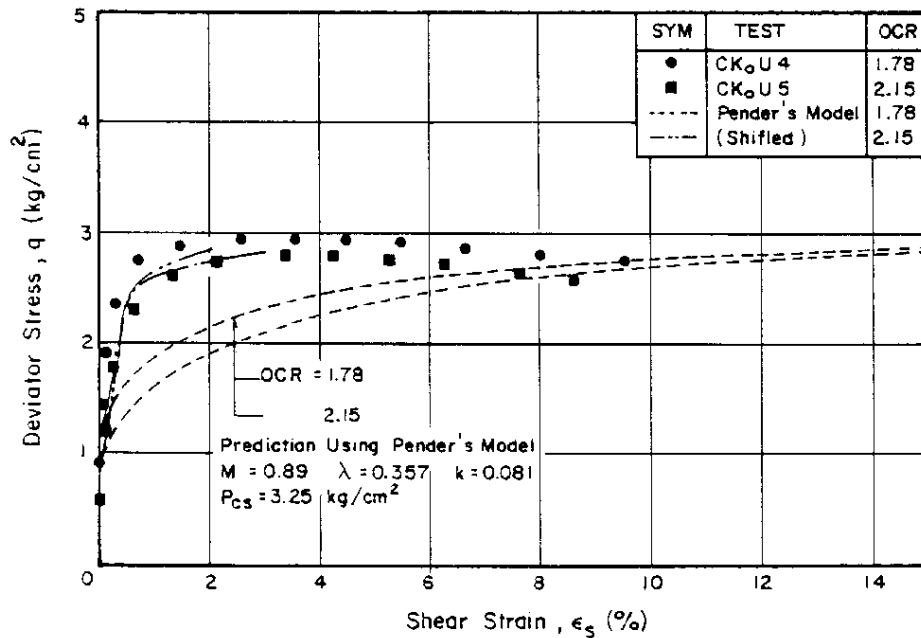


**Fig. 36 ( $q, \epsilon_s$ ) Plot for  $K_0$ -overconsolidated Samples Compared with the Predictions from Pender's Model with and without Shifted Initial Stress Points (Dry Zone)**

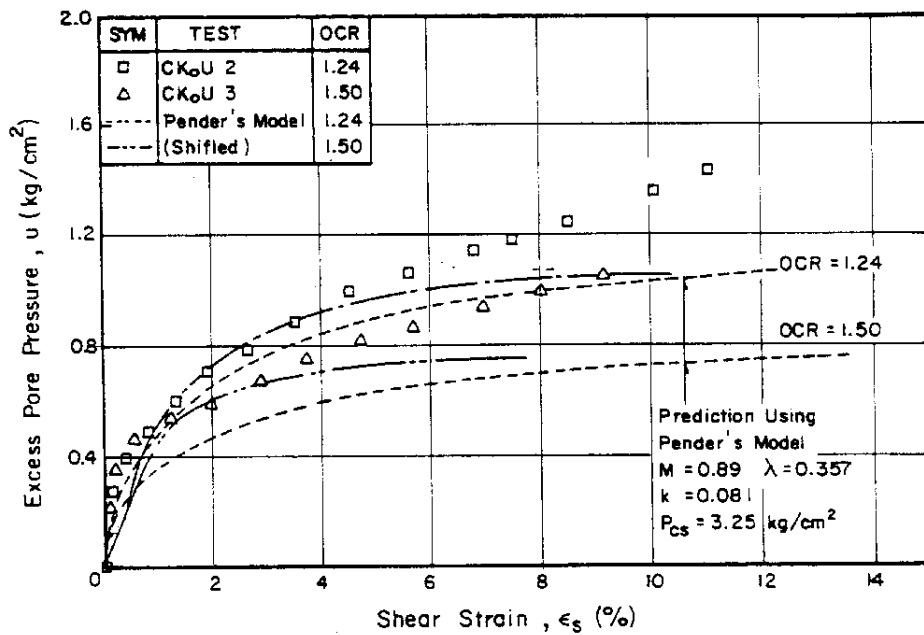


**Fig. 37** ( $u, \epsilon_s$ ) Plot for  $K_0$ -overconsolidated Samples Compared with the Predictions from Pender's Model with and without Shifted Initial Stress Points (Wet Zone)

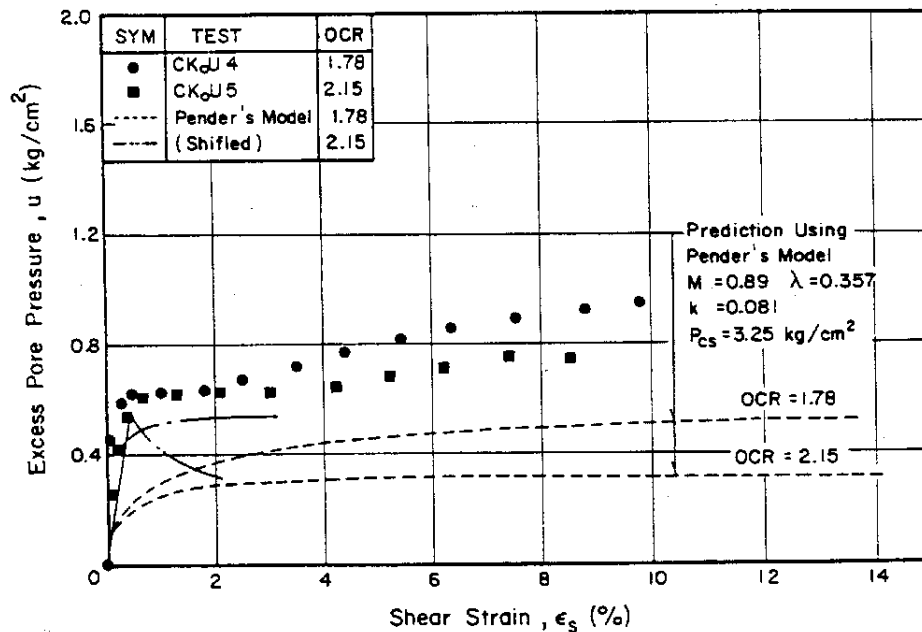


**Fig. 38** ( $u, \epsilon_s$ ) Plot for  $K_0$ -overconsolidated Samples Compared with the Predictions from Pender's Model with and without Shifted Initial Stress Points (Dry Zone)

## CRITICAL STATE MODELS

peak deviator stress conditions. However, this model overpredicts the shear strains both for the isotropically consolidated and for the  $K_o$ -consolidated samples.

### Drained Behavior of Normally Consolidated Samples

1. **Pender's Model** - Pender's Model overpredicts the strains for the  $CK_oD$  and  $CK_oDE$  tests. This model, however, gives good predictions of the volumetric strain both in compression and in extension.
2. **Dafalias' Model** - For the  $CK_oD$  type of loading, this model predicted the  $(q, \epsilon_s)$  and  $(q, \epsilon_v)$  relationships well.
3. **Atkinson et al.'s Model** - This model overpredicts shear and volumetric strains for the  $CK_oD$  type of loading.

### Drained Behavior of Overconsolidated Samples

**Pender's Model** - Pender's Model is found to overpredict shear strains in most cases. The deviations become more and more apparent when the OCR values are increased. However, this model gives excellent predictions of the volumetric strains for the overconsolidated samples under compression types of loading. It can be concluded that Pender's Model, for the overconsolidated behavior, overpredicts the shear strain both in undrained and in drained tests. This is attributed partially or fully to the incorrect assumption made on the plastic strain increment ratio in the formulation of the theory.

### Improvement of Pender's Model

The OCR value or related parameter can be a possible reduction factor to be applied to the assumption of the plastic strain increment ratio for the lightly overconsolidated samples ( $OCR < 3.0$ ). Pender's hypotheses on the shapes of the undrained stress path for the  $K_o$  overconsolidated sample is found to be an oversimplification. Thus, the prediction of Pender's Model for  $K_o$  overconsolidated samples is expected to be promising when this factor is incorporated in the expression for the plastic strain increment ratio.

## REFERENCES

- ATKINSON, J. H.; RICHARDSON, D.; and ROBINSON, P. J. (1987). Compression and extension of  $K_o$  normally consolidated Kaolin clay, *Journal of Geotechnical Engineering Division*, ASCE, Vol. 113, No. 12, pp. 1468-148

*KIM, LIN, BERGADO, and BALASUBRAMANIAM*

- BALASUBRAMANIAM, A. S. (1969). Some factors influencing the stress-strain behavior of clays, Ph. D. Thesis, Cambridge University, Cambridge.
- BURLAND, J. B. (1965). The yielding and dilation of clay, Correspondence, *Geotechnique*, Vol. 15, No. 2, pp. 211-214.
- CHANG, M. F. (1973). A rational method for determining the in-situ coefficient of earth pressure at rest, M. Eng. Thesis, No. 510, AIT, Bangkok, Thailand.
- CHAIYADHUMA, W. (1974). Undrained shear strength characteristics of Nong Ngoo Hao soft clay under  $K_0$ -anisotropic consolidation, M. Eng. Thesis, No. 698, Asian Institute of Technology, Bangkok, Thailand.
- DAFALIAS, Y. F. (1987). An anisotropic critical state clay plasticity model. *Constitutive Laws for Engineering Materials Theory and Applications*, Vol. 1, pp. 513-522.
- LADD, C. C.; FOOTT, R.; ISHIHARA, K.; SCHLOSSER, F.; and POULOS, H. G. (1977), Stress-deformation and strength characteristics: State-of-the-art report, *Proceedings of the Ninth International Conference on Soil Mechanics and Foundation Engineering*, Vol. 2, Tokyo, Japan, pp. 421-494.
- PENDER, M. J. (1977), A unified model for soil stress- strain behavior. *Proceedings of the Tenth International Conference on Soil Mechanics and Foundation Engineering*, Specialty Session No. 9, Constitutive Equation of Soils, Tokyo, Japan, pp. 213-222,
- PENDER, M. J. (1978). A model for behavior of overconsolidated soil, *Geotechnique*, Vol. 28, No. 1, pp. 1-25.
- ROSCOE, K. H. and BURLAND, J. B. (1968). On the generalized stress-strain behavior of wet clay, *Engineering Plasticity*, Cambridge: Cambridge University Press, pp. 535-609.
- WONG, P. K. K. and MITCHELL, R. J. (1975). Yielding and plastic flow of sensitive clay. *Geotechnique*, Vol. 25, No. 4, pp. 763-782.